FC

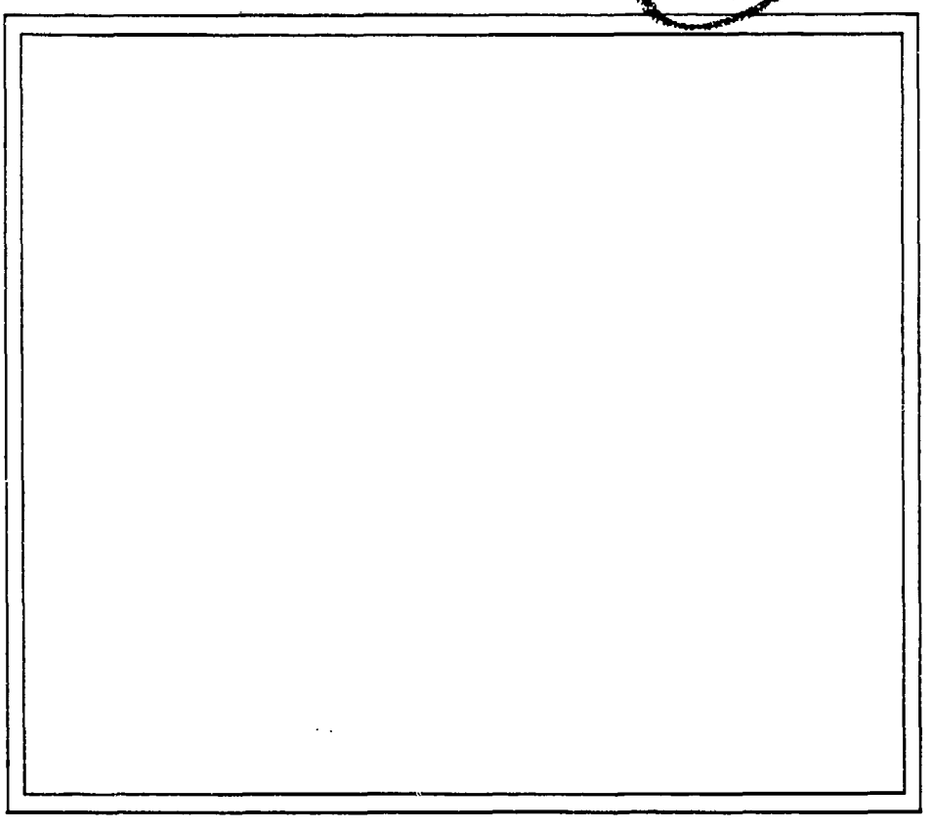

PRINCETON UNIVERSITY
Department of Civil Engineering

Technical Report No. 45
Civil Engng. Res. Report No. 77-SM-1

CONTINUUM MECHANICS AT THE ATOMIC SCALE

by

A. Cemal Eringen

Research Sponsored by the
Office of Naval Research

under

Contract N00014-76-C-0240
Task Number NR 064-410

January 1977

SECURITY CLASSIFICATION OF THIS PAGE *(When Data Entered)*

REPORT DOCUMENTATION PAGE

READ INSTRUCTIONS BEFORE COMPLETING FORM

1. REPORT NUMBER: Technical Report No. 45
2. GOVT ACCESSION NO.
3. RECIPIENT'S CATALOG NUMBER (9)
4. TITLE *(and Subtitle)*: (6) Continuum Mechanics at the Atomic Scale
5. TYPE OF REPORT & PERIOD COVERED: Technical Report
6. PERFORMING ORG. REPORT NUMBER: (14) 77-SM-1, TR-45
7. AUTHOR(s): (10) A. Cemal Eringen
8. CONTRACT OR GRANT NUMBER(s): (15) N00014-76-C-0240
9. PERFORMING ORGANIZATION NAME AND ADDRESS: Civil + Geological Engineering, Princeton University, Princeton, NJ 08540 — 401 272
10. PROGRAM ELEMENT, PROJECT, TASK AREA & WORK UNIT NUMBERS: NR-064-410
11. CONTROLLING OFFICE NAME AND ADDRESS
12. REPORT DATE: (11) January 1977
13. NUMBER OF PAGES: 58 pages
14. MONITORING AGENCY NAME & ADDRESS *(if different from Controlling Office)*: (12) 61 p.
15. SECURITY CLASS. *(of this report)*: Unclassified
15a. DECLASSIFICATION/DOWNGRADING SCHEDULE
16. DISTRIBUTION STATEMENT *(of this Report)*

17. DISTRIBUTION STATEMENT *(of the abstract entered in Block 20, if different from Report)*

Approved for public release; Distribution Unlimited

18. SUPPLEMENTARY NOTES

19. KEY WORDS *(Continue on reverse side if necessary and identify by block number)*

nonlocal continuum mechanics
crack tip problem
fracture mechanics
screw dislocation
secondary flow in pipes

20. ABSTRACT *(Continue on reverse side if necessary and identify by block number)*

The recent theories of nonlocal continuum mechanics are summarized and applied to the problems of plane waves, crack tip, screw dislocations, and secondary flow in rectangular pipes. The power and potential of these theories are demonstrated by predicting various critical physical phenomena in the range from the global to the atomic scales.

DD FORM 1 JAN 73 1473 EDITION OF 1 NOV 63 IS OBSOLETE
S/N 0102-014-6601

SECURITY CLASSIFICATION OF THIS PAGE *(When Data Entered)*

401272

CONTINUUM MECHANICS AT THE ATOMIC SCALE*

A. Cemal Eringen
Princeton University

CONTENTS

*Engineering Science Lecture presented at the 13th Annual Meeting of the Society of Engineering Science, Inc., NASA Headquarters, Hampton, Virginia, November 2, 1976

CONTINUUM MECHANICS AT THE ATOMIC SCALE[1]

A. Cemal Eringen
Princeton University

ABSTRACT

The recent theories of nonlocal continuum mechanics are summarized and applied to the problems of plane waves, crack tip, screw dislocations, and secondary flow in rectangular pipes. The power and potential of these theories are demonstrated by predicting various critical physical phenomena in the range from the global to the atomic scales.

1. INTRODUCTION

In all branches of the classical field theories, the ultimate desire is to determine certain fields (e.g., displacement, velocity, stress, electric field, etc.) at a spatial point $\underset{\sim}{x}$ at time t. The differential field equations constructed are solved under appropriate boundary and initial conditions as functions of four variables $\underset{\sim}{x}$ and t. For the existence and uniqueness of solutions, certain smoothness requirements are placed on the geometry of the body and the initial and boundary conditions. Within this scheme, the solutions obtained have served useful purposes in engineering and physical applications, stimulated many mathematical developments and extensive experimental work. However, practitioners, often too busy with the difficulties

[1]This work was partially supported by the Office of Naval Research and the Army Research Office-Durham.

of problems at hand, have forgotten or disregarded the underlying assumptions of the classical field theories that make these theories inapplicable to their problems. When such efforts did not bear fruit (as it is natural that they should not) then a "patch work" was made to mend some part of the field equation with arbitrary parameters and functions so that the result can be brought within the vicinity of experiments for that particular problem. Such situations are well-known, for example, consider the plethora of theories of turbulence, creep, fatigue and fracture of solids, dispersion and absorption of E-M waves, etc. These approaches, too, having some convincing power, proliferated the literature with so much material that even the proponents or worshippers of the one-dimensional world seem to express some despair in mastering a given field.

For a mathematical field quantity (e.g., a scalar, vector or tensor) to represent a physical field (e.g., free energy, stress, electric field) clearly certain conditions must be satisfied. Basic to these conditions are the length and/or time requirements which arise from the discrete inner structure of bodies and the inner transmission time of signals. All materials are made up of some *subbodies* (atoms, molecules, grains) which are attracted to each other by interatomic forces. Whatever may be the scale, be it the atomic, molecular or a much larger scale of grains and gross structure, we can associate an *inner characteristic* length λ with a given body. This may be taken to be the atomic distance or the granular distance depending on the nature of the physical phenomena sought. In theories that can account for the atomic scale phenomena, we may take λ as the atomic distance, and for granular, porous or composite materials typical size or distance of *subbodies* constituting the body (e.g., grain size, pore size, average distance of fibers in a composite). In addition, with these subbodies, there is associated a time scale τ (or frequency ω) which may be the minimum transmission time of a signal (or an associated frequency) from one subbody to the next. In some cases, this may be taken to be an atomic or molecular relaxation time (or a related frequency). Associated with the external stimuli (e.g., waves, distances over which load distributions change sharply) and geometrical and surface discontinuities (e.g., cracks, sharp notches, corners) is an external characteristic length ℓ and time t_o (or frequency w_o). The domain of applicability of a continuum theory depends on the ratios

$$\left(\frac{\lambda}{\ell} \quad , \quad \frac{\tau}{t_o} \left(\text{or } \frac{w_o}{\omega} \right) \right)$$

For $\lambda/\ell << 1$, $\tau/t_o << 1$ the external stimuli excites large numbers of subbodies simultaneously so that the subbodies act cooperativley and the outcome is a statistical average of the individual responses. The individual characteristics of subbodies are unimportant and the field concept at a point (e.g., at the center of mass of a group of subbodies) make sense. The field associated with this point is the average field of a subbody. On the other hand, if $\lambda/\ell \simeq 1$, $\tau/t_o \simeq 1$ the individual fields of subbodies are important and the collaborative action of subbodies are influenced by their individual responses substantially.[2] In this case, clearly the intermolecular and atomic forces are important so that the relative motion of a distant atom influences the behavior of any other atom. This is the case where intermolecular distant forces and their distributions over space and time are essential in the outcome.

All classical field theories intrinsically assume that $\lambda/\ell << 1$ and generally[3] $\tau/t_o << 1$. Clearly, we cannot expect a reasonable treatment of physical phenomena in which these conditions are violated. In fact, this turns out to be the case for many important classes of physical problems among which we cite: the transmission of waves with small wave lengths (or high frequency waves) state of stress at a crack tip or dislocation core, generation of secondary flow in pipes, turbulence, all physical phenomena associated with the surface of a body, fracture of solids, microcrack growth, fatigue, dispersion E-M waves, the so-called negative dielectric, etc. To deal with these problems, we must either revert to the use of atomic theories (e.g., lattice dynamics) or develop theories that can reach the atomic and molecular regions.

Phonon dispersion experiments with perfect crystals indicate clearly that the high frequency waves are dispersive and the speed of propagation of these waves diminishes to zero as the wave length ℓ approaches the atomic dimension a. Classical elasticity near the infinite wave lengths predicts correct phase velocity, but it fails in the short wave length regions and predicts no dispersion at all. For perfect crystals with no surfaces, the atomic lattice dynamics gives excellent results in the

---

[2] Often $\lambda/\ell \simeq 1$ implies $\tau/t_o \simeq 1$ in many materials. However, important cases exist in which $\lambda/\ell << 1$, $\tau/t_o \simeq 1$ (e.g., polymeric materials). Conversely, we may have $\lambda/\ell \simeq 1$ but $\tau/t_o << 1$. Such is the case for many perfect crystals.

[3] $\tau/t_o << 1$ is violated for memory dependent materials (e.g., polymeric substances, viscoelastic materials).

entire Brillouin zone (from $\ell=\infty$ to $\ell=a$). Thus the question arises: why not use the lattice dynamics and forget about the field theories. The reason for not doing this is two-fold:

(a) Real materials, unlike perfect crystals, are too complicated in their inner structures. Imperfections, impurities, dislocations, holes, microcracks are too widespread.

(b) Inter-atomic forces are too complicated and by-in-large they are unknown even in their distributions

These two facts, when combined with the colossal number of differential equations,[4] make it nearly impossible to employ the atomic theory for real materials even with the faster computers available today. The cost is prohibitive in all cases (especially when quantum effects need be taken into account).

In a realistic problem, the individual behavior of each atom in the body is often unimportant. We are interested in the response of the body to given stimuli within an experimentally possible length and time scale. Thus the practical domain of applicability of a theory is determined by the smallest size of probes used in experimentations. Nevertheless, one may be forced to construct theories beyond this range in order to obtain accuracies within the experimental ranges. Moreover, approximations are always more meaningful when one starts with "exact" theories. It is, therefore, clear that in the range between the infinite wave length and a wave length of one atomic distance, there lies the genuine, intriguing and real problems of materials. This region is impossible to penetrate by the use of the classical field theories and very difficult to cover with the atomic lattice dynamics. The raison d'être of continuum mechanics at the atomic scale may be summarized as:

(i) Prediction and control of physical phenomena triggered by long range forces;

(ii) Imperfect and complicated inner structures of real materials;

(iii) Inclusion of the surface physics;

(iv) Difficulty and cost of calculations based on atomic models. Inherent in these calculations is the production of the unnecessarily large amounts of costly data.

(v) Lack of knowledge of the atomic geometry and force fields.

With such a critique, one may sets one's standard on too high a scale and expect from a continuum theory the capability for the treatment

---

[4] For Newtonian theory, 3N second order nonlinear ordinary differential equations, where N is the number of the atoms in a body.

of some impossible problems. We must note that a continuum theory being a field theory still involves continuous fields over a reasonable distance and time. Thus, it will represent an approximation to the atomic theory with the hope that perhaps averages are now based on smaller distances in the neighborhood of the atomic distance (for example, 50 to 100 atomic distances). If achieved, this would represent a major breakthrough over the classical continuum theories which fail long before such a scale is reached.

In this article, I would like to discuss briefly the recently developed nonlocal continuum theory and present several solutions of some critical problems that hitherto defied any rational treatment. The mathematical formulations of the theory and details of the solutions of these problems have been and are being published elsewhere (see references). The main purpose of this article is to expose the fundamental physical ideas underlying the nonlocal theory and to demonstrate the potential of the theory via the solution of various problems that fall outside of the classical field theories. In Section 2, we present the balance laws and jump conditions. Section 3 is devoted to a sketch of the constitutive theory. Section 4 is concerned with the propagation of plane waves and the determination of the nonlocal material moduli. In Section 5, we discuss the problem of crack tip and develop a natural fracture criteria which unifies, in a most natural way, the global fracture criteria used in engineering and Griffith's criterion used in the fracture of solids. Section 6 contains the solution of a basic dislocation problem, namely the screw dislocation. In Section 7, we turn our attention to some problems in fluid dynamics, in particular, to the generation of secondary flow in pipes of rectangular cross section. The final section briefly mentions the prospects for the nonlocal theory.

2. BALANCE LAWS OF NONLOCAL CONTINUUM MECHANICS

The global balance laws of nonlocal continuum mechanics are identical to those of classical continuum mechanics. Thus, the balance laws for the entire body with volume V enclosed by a surface ∂V are expressed as:

$$\frac{d}{dt}\int_{V-\sigma} \Phi \, dv - \int_{\partial V-\sigma} \underset{\sim}{\tau}\cdot d\underset{\sim}{a} - \int_{\partial V-\sigma} g \, dv = 0 \qquad (2.1)$$

where σ is a discontinuity surface sweeping the body with a velocity $\underset{\sim}{v}$ in the direction of its unit normal $\underset{\sim}{n}$, Fig. 1. Equation (2.1) states that

the time rate of change of the total field Φ in the body, excluding the points of V which are on $\sigma(V\text{-}\sigma)$, is balanced with the surface flux $\underset{\sim}{\tau}$ of Φ and body source g. By the use of the Green-Gauss theorem one may then transform the integral over $\partial V\text{-}\sigma$ and carry out the time rate to obtain (cf., Eringen [1967], p. 77).

$$\int_{V-\sigma} \left[\frac{\partial \Phi}{\partial t} + \operatorname{div}(\Phi \underset{\sim}{v} - \underset{\sim}{\tau}) - g\right] dv + \int_{\sigma} [\![\Phi(\underset{\sim}{v} - \underset{\sim}{v}) - \underset{\sim}{\tau}]\!] \cdot d\underset{\sim}{a} = 0 \tag{2.2}$$

where $\underset{\sim}{v}$ is the velocity vector and a bold-face bracket represents the jump of its enclosure at σ. In the classical field theories, a strong assumption is made, namely: (2.2) is considered to be valid for every part of the body however small it may be. It then follows that the integrands of the two integrals in (2.2) must vanish. This is called localization. In the nonlocal theory we abandon this strong assumption. Nevertheless, the localization is still possible by writing the equivalent set

$$\frac{\partial \Phi}{\partial t} + \operatorname{div}(\Phi \underset{\sim}{v} - \underset{\sim}{\tau}) - g = \hat{g} \qquad \text{in } V\text{-}\sigma \tag{2.3}$$

$$[\![\Phi(\underset{\sim}{v} - \underset{\sim}{v}) - \underset{\sim}{\tau}]\!] \cdot \underset{\sim}{n} = \hat{G} \qquad \text{on } \sigma \tag{2.4}$$

subject to

$$\int_{V-\sigma} \hat{g}\, dv + \int_{\sigma} \hat{G}\, da = 0 \tag{2.5}$$

Thus, the nonlocal theory contains certain *residuals* (carrying a hat "^") which must integrate to zero. These residuals are the effects of all other points of the body on the point under consideration. The determination of these residuals is an integral part of the theory.

The master balance laws (2.3) to (2.5) may be used to obtain specific balance laws. We list only the volume part (eq. 2.3) for mass, momentum, moment of momentum and energy (cf., Erignen [1972a,b], [1976a], Eringen and Edelen [1972]).

$$\frac{\partial \rho}{\partial t} + \operatorname{div}(\rho \underset{\sim}{v}) = \hat{\rho} \tag{2.6}$$

$$\operatorname{div} \underset{\sim}{t}_k + \rho(\underset{\sim}{f} - \dot{\underset{\sim}{v}}) = \hat{\rho} \underset{\sim}{v} - \rho \hat{\underset{\sim}{f}} \tag{2.7}$$

$$\underset{\sim}{l}_k \times \underset{\sim}{t}_k - \rho(\underset{\sim}{x} \times \hat{\underset{\sim}{f}} - \hat{\underset{\sim}{\ell}}) = \underset{\sim}{0} \tag{2.8}$$

$$-\rho\dot{\varepsilon} + \underset{\sim}{t}_k \cdot \underset{\sim}{v}_{,k} + \underset{\sim}{\nabla}\cdot\underset{\sim}{q} + \rho h - \hat{\rho}(\varepsilon - \tfrac{1}{2}v\cdot v) - \rho\hat{\underset{\sim}{f}}\cdot\underset{\sim}{v} + \rho\hat{h} = 0 \qquad (2.9)$$

where a subscript following a comma indicates a partial derivative and a superposed dot a material time derivative, e.g.,

$$\underset{\sim}{v}_{,k} \equiv \frac{\partial \underset{\sim}{v}}{\partial x_k} \quad , \qquad \dot{\varepsilon} \equiv \frac{d\varepsilon}{dt}$$

and

$\rho \equiv$ mass density , $\hat{\rho} \equiv$ mass residual

$\underset{\sim}{t}_k \equiv t_{k\ell}\underset{\sim}{1}_\ell$ = stress vectors , $\hat{\underset{\sim}{f}} \equiv$ body force residual

$\underset{\sim}{1}_k \equiv$ cartesian unit vectors , $\hat{\underset{\sim}{\ell}}$ = body couple residual

ε = internal energy density , $\hat{h}$ = energy residual

$\underset{\sim}{q}$ = the heat vector.

The residuals are subject to[5]

$$\int_V (\hat{\rho}, \rho\hat{\underset{\sim}{f}}, \rho\hat{\underset{\sim}{\ell}}, \rho\hat{h})\, dv = 0 \qquad (2.10)$$

Equation (2.3) with the equality sign (=) replaced by ($\geq$) can be used to obtain the second law of thermodynamics

$$\rho\dot{\eta} - \underset{\sim}{\nabla}\cdot\underset{\sim}{q} - \frac{\rho h}{\theta} - \rho\hat{b} + \hat{\rho}\eta \geq 0 \qquad \text{in } V-\sigma \qquad (2.11)$$

where η is the entropy density, θ is the absolute temperature and $\hat{b}$ is entropy residual subject to

$$\int_{V-\sigma} \rho\hat{b}\, dv = 0 \qquad (2.12)$$

The balance laws (2.6) to (2.9) and the second law of thermodynamics (2.11) are valid for all bodies irrespective of their constitutions and geometries (e.g., fluids, solids, blood, polymers, crystals). We now face a major task of not only establishing appropriate constitutive equations for bodies of different constitutions but also of determining the forms of the residuals. Various expositions of the theories are given in some of our previous works (cf., Eringen [1972b,c], [1974a,b,c], [1973a], [1976a,b,c].

[5] Assuming the total surface residuals vanish separately.

Alternative approaches to nonlocal elasticity employing variational and/or quasi-continuum methods exist (cf., Kröner [1967], Krumhansl [1965, 1968], Regula [1965], Kunin [1966a,b, 1967a,b, 1968]). Continuum Physics, Vol. IV, Eringen [1976a] contains a more extensive and up-to-date literature and various expositions of the nonlocal continuum theories.

In Section 3, we present the basic ideas underlying the constitutive theory and some elementary results.

3. CONSTITUTIVE EQUATIONS

The characterization of the material properties are made through the constitutive equations. As in the classical field theories we condider as the *independent variables the motions and temperatures of all points of the body at all past times.* The dependent variables are the stress $\underset{\sim}{t}$, heat $\underset{\sim}{q}$, energy ε and the entropy η. The nonlocal residuals must also be incorporated into this group. These quantities are then considered to be *functionals* depending on the motions and temperature histories of *all* points of the body. It is clear that no longer Euclidean space is adequate for the description of the constitutive functionals. It is found that a Banach space or more usefully a Hilbert space is most appropriate for this purpose. Here we outline briefly the situation for the nonlocal elastic solids. The nonlocal fluids are discussed briefly in Section 7. For a thorough discussion of constitutive equations, see Eringen [1972b,c], Eringen and Edelen [1972], [1974a,b,c], [1976a].

3.1 Nonlocal Memory Dependent Materials

The constitutive equations of nonlocal memory dependent materials are of the form

$$\rho_o \psi = \Sigma(\underset{\sim}{x}', \underset{\sim}{x}'_{,k}, \theta', \theta_{,k}) \tag{3.1}$$

where ρ_o is the density in the natural state V referred to a rectangular frame of reference X_K, K=1,2,3, $\psi \equiv \varepsilon - \theta\eta$ is the *free energy* functional, $\underset{\sim}{x} = \underset{\sim}{x}(\underset{\sim}{X},t)$ represents the motion of the material point $\underset{\sim}{X}$ at time t (i.e., the spatial point $\underset{\sim}{x}$ occupied by the material point $\underset{\sim}{X}$ at time t). As usual the axiom of continuity is posited, i.e., the inverse motion $\underset{\sim}{X} = \underset{\sim}{X}(\underset{\sim}{x},t)$ is assumed to exist and is the unique inverse of $\underset{\sim}{x} = \underset{\sim}{x}(\underset{\sim}{X},t)$ at all points of the body. A prime placed on quantities indicates that they depend on $\underset{\sim}{X}'$ and $t' \leq t$ where $\underset{\sim}{X}'$ represents any other point in the body and t' any time at or prior to the present time t. Σ in (3.1) is a *functional* over all argument functions of $\underset{\sim}{X}'$ covering the entire body and all past times t'.

Equations similar to (3.1) are also written for the stress tensor, heat vector, and entropy residuals.

We group the independent variables as an ordered set

$$\underset{\sim}{F}' = \{\underset{\sim}{x}', \theta', \underset{\sim}{x}'_{,K}, \theta'_{,K}\} \tag{3.2}$$

and define the inner product of any two such sets by

$$(\underset{\sim}{F}'_1, \underset{\sim}{F}'_2)_H = \int_{V-\Sigma} H(|\underset{\sim}{X}'-\underset{\sim}{X}|)\underset{\sim}{F}_1(\underset{\sim}{X}')\cdot\underset{\sim}{F}_2(\underset{\sim}{X}')dV(\underset{\sim}{X}') \tag{3.3}$$

where

$$\underset{\sim}{F}'_1\cdot\underset{\sim}{F}'_2 = \underset{\sim}{x}'_1\cdot\underset{\sim}{x}'_2 + \theta'_1\theta'_2 + \underset{\sim}{x}'_{1,K}\cdot\underset{\sim}{x}'_{2,K} + \theta'_{1,K}\,\theta'_{2,K} \tag{3.4}$$

and $H(|\underset{\sim}{X}'-\underset{\sim}{X}|)$, called the *influence function*, is a positive decreasing function of $|\underset{\sim}{X}'-\underset{\sim}{X}|$ such taht $H(0) = 1$. The inner product (3.3) naturally induces a norm $(\underset{\sim}{F}',\underset{\sim}{F}')_H$ in a Hilbert space H. We are now able to assume continuity and differentiability of the constitutive functionals, such as Σ. After eliminating h between (2.11) and (2.9) and writing $\varepsilon = \psi+\theta\eta$, we obtain the generalized Clausius-Duhem inequality

$$-\frac{\rho}{\theta}(\dot{\psi}+\dot{\theta}\eta) + \frac{1}{\theta}\,\underset{\sim}{t}_k\cdot\underset{\sim}{v}_{,k} + \frac{1}{\theta^2}\,\underset{\sim}{q}\cdot\underset{\sim}{\nabla}\theta - \frac{\hat{\rho}}{\theta}(\psi-\tfrac{1}{2}\underset{\sim}{v}\cdot\underset{\sim}{v}) - \frac{\rho}{\theta}\,\hat{\underset{\sim}{f}}\cdot\underset{\sim}{v}$$
$$+\frac{\rho}{\theta}\,\hat{h} - \rho\hat{b} \geq 0 \qquad , \qquad \text{in } V-\sigma \tag{3.5}$$

This inequality must not be violated for all independent thermomechanical processes. With the apparatus of Hilbert space, we can now calculate $\dot{\psi}$ and substitute into (3.5). The inequality so obtained can be used to derive some important results. The process is lengthy and tedious but the outcome is elegant and meaningful. Leaving out the details, we give below the results for elastic solids (no memory dependence, i.e., t' is replaced by t).

3.2 Nonlocal Elastic Solids

Theorem. The constitutive equations of the nonlocal elastic solids and residuals do not violate the global entropy inequality if and only if they are of the form (cf., Eringen [1976a, p. 221]).

$$
\begin{aligned}
T_{Kk} &= \rho_o \frac{\partial \psi}{\partial x_{k,K}} + \int_{V-\Sigma} \left(\rho_o \frac{\delta \psi}{\delta x'_{k,K}} \right)^* dV(\underset{\sim}{\Lambda}) \\
\rho_o \eta &= -\rho_o \frac{\partial \psi}{\partial \theta} - \int_{V-\Sigma} \left(\rho_o \frac{\delta \psi}{\delta \theta'} \right)^* dV(\underset{\sim}{\Lambda}) \\
\underset{\sim}{q} &= \underset{\sim}{0} \\
\rho_o \hat{f}_k &= -\rho_o \frac{\partial \psi}{\partial x_k} - \int_{V-\Sigma} \left(\rho_o \frac{\delta \psi}{\delta x'_k} \right)^* dV(\underset{\sim}{\Lambda}) \\
\hat{\rho} &= 0
\end{aligned}
\tag{3.6}
$$

where $T_{Kk} = \frac{\rho_o}{\rho} t_{\ell k} X_{K,\ell}$ is the Piola stress. The integration is over the entire volume at the natural state excluding the discontinuity surface Σ, $\delta\psi/\delta(\ )$ indicates the Fréchet partial derivative, and an asterisk placed on parentheses represents the interchange of $\underset{\sim}{\Lambda}$ and $\underset{\sim}{X}$, i.e.

$$
[G(\underset{\sim}{\Lambda}, \underset{\sim}{X})]^* = G(\underset{\sim}{X}, \underset{\sim}{\Lambda})
$$

where $\underset{\sim}{\Lambda}$ is the auxilliary vector variable arising from the Fréchet derivative. It is interesting that the thermodynamic admissibility requires the nonlocal mass residual vanish. Note that the first two terms in the expressions of T_{Kk} and $\rho_o \eta$ are the classical terms and the nonlocality introduces the volume integrals.

The axiom of objectivity further restricts these equations. It can also be shown that the integral of $\rho_o \hat{\underset{\sim}{f}}$ over $V-\Sigma$ vanishes, as demanded by (2.10).

With this sketchy account, leaving out many of the interesting details and results in the nonlinear theory, we copy the constitutive equations of *linear homogeneous and isotropic nonlocal elastic solids* from Eringen [1972b, see also 1976a, p. 245].

$$
\begin{aligned}
t_{k\ell} &= \lambda e_{rr} \delta_{k\ell} + 2\mu e_{k\ell} + \int_{V-\sigma} (\lambda'_1 e'_{rr} \delta_{k\ell} + 2\mu'_1 e'_{k\ell}) dv' \\
\Sigma &= \Sigma_o + \tfrac{1}{2}\lambda (e_{kk})^2 + \mu e_{k\ell} d_{k\ell} + \int_{V-\sigma} \frac{\lambda'_1}{2} e_{kk} e'_{\ell\ell} + \mu'_1 e_{k\ell} e'_{k\ell} \, dv' \\
\hat{f}_k &= 0 \quad , \quad \hat{\rho} = 0
\end{aligned}
\tag{3.7}
$$

where $e_{k\ell}$ is the strain tensor of the linear theory

$$e_{k\ell} = \tfrac{1}{2}(u_{k,\ell} + u_{\ell,k}) \tag{3.8}$$

in which $u_k(\underset{\sim}{x},t)$ is the displacement vector. In (3.7) λ and μ are the classical Lame constants and λ_1' and μ_1' are functions of $|\underset{\sim}{x}'-\underset{\sim}{x}|$. A more convenient form of (3.7) is

$$t_{k\ell} = \int_{V-\sigma} [\lambda'(|\underset{\sim}{x}'-\underset{\sim}{x}|)e'_{rr}(\underset{\sim}{x}')\delta_{k\ell} + 2\mu'(|\underset{\sim}{x}'-\underset{\sim}{x}|)e'_{k\ell}(\underset{\sim}{x}')]d\upsilon(\underset{\sim}{x}')$$

$$\Sigma = \Sigma_o + \int_{V-\sigma} (\tfrac{1}{2}\lambda' e_{kk}e'_{\ell\ell} + \mu'\epsilon_{k\ell}e'_{k\ell})d\upsilon' \tag{3.9}$$

which incorporates λ and μ into λ' and μ'.

3.3 Field Equations

Upon carrying $(3.9)_1$ into (2.7), and since $\hat{\rho}$ and $\hat{\underset{\sim}{f}}$ vanish in the linear theory, we obtain

$$\int_{V-\sigma} [(\lambda' + 2\mu')\underset{\sim}{\nabla}'\underset{\sim}{\nabla}'\cdot\underset{\sim}{u} - \mu'\nabla'x\nabla'x\underset{\sim}{u}']d\upsilon'$$

$$- \int_{\partial V-\sigma} \underset{\sim}{T}'_k \, da_k + \int_{\sigma} [\underset{\sim}{T}'_k] \, da'_k + \rho(\underset{\sim}{f}-\ddot{\underset{\sim}{u}}) = \underset{\sim}{0} \tag{3.10}$$

where

$$\underset{\sim}{T}'_k = T'_{k\ell}\underset{\sim}{1}_\ell \quad , \qquad T'_{k\ell} \equiv \lambda' e'_{rr}\delta_{k\ell} + 2\mu' e'_{k\ell} \tag{3.11}$$

The surface integrals in (3.10) result from using the Green-Gauss theorem after replacing $\partial\lambda'/\partial x_k$ by $-\partial\lambda'/\partial x'_k$.

The integro-partial differential equations (3.10) are the basic field equations of the linear, homogeneous, isotropic, nonlocal elastic solids. We note the interesting surface terms containing $T'_{k\ell}$. These terms represent *surface stresses* (e.g., surface tension) not included in the classical theory. Thus *the nonlocal theory includes the surface physics* which is not accounted for in the classical field theories.

We are now ready to test the theory.

4. PROPAGATION OF PLANE WAVES

The displacement field $u_1 = u(x,t)$, $u_2 = u_3 = 0$ of a plane, longitudinal wave propagating in the $x_1 \equiv$ x-direction may be represented by the Fourier integral

$$u(x,t) = \frac{1}{2\pi} \int_{-\infty}^{\infty} \bar{u}(\xi,\omega) \exp\,[-i(\xi x + \omega t)]\, d\xi\, d\omega \tag{4.1}$$

where $\bar{u}(\xi,\omega)$ is the Fourier transform of $u(x,t)$. Since the body has no surface and $\underset{\sim}{f}=\underset{\sim}{0}$, the field equations (3.10) in the one-dimensional case take the form

$$\int_{-\infty}^{\infty} (\lambda' + 2\mu') \frac{\partial^2 u'}{\partial x'^2}\, dx' - \rho \frac{\partial^2 u}{\partial t^2} = 0 \tag{4.2}$$

The Fourier transform of this gives

$$\omega^2/c_1^2 = \bar{\alpha}(\xi)\xi^2 \tag{4.3}$$

where $\bar{\alpha}$ is the Fourier transform of $\alpha(x)$ defined by

$$\alpha(x) \equiv \frac{\lambda'+2\mu'}{\lambda+2\mu} \tag{4.4}$$

and $c_1 \equiv \left(\frac{\lambda+2\mu}{\rho}\right)^{1/2}$ is the phase velocity of the longitudinal waves in classical elasticity. For the classical limit $\bar{\alpha}=1$ and therefore the elastic waves are non-dispersive. From (4.3) it is clear that nonlocal elasticity predicts dispersive waves.

In the lattice dynamics, it is well-known that the elastic waves are dispersive and the dispersion curves within one Brillouin zone (the wave length between the atomic distance a and infinity) are typically as shown in Figures 2,3. In these figures, the dispersion curves for the transverse waves are also shown. There exists a simple one-dimensional lattice dynamics model which consists of a chain of atoms of mass M attached to each other by linear springs of equal length, Figure 4. This model, known as the Born-Kármán model, is based on nearest neighbor interactions. The dispersion relations for this model is found to be (cf., Brillouin [1953, p. 4]), Figure 5,

$$\omega^2/c_1^2 = \frac{4}{a^2} \sin^2(\xi a/2) \tag{4.5}$$

where a is the atomic distance. It is clear that such a model, even though it is crude, is much more realistic than the classical elasticity for wave

numbers (ξ) close to the atomic distances. Of course, at $\xi=0$ (infinite wave length) (4.5) gives the same result known in classical elasticity. Thus, if we wish the nonlocal theory to give identical results to the atomic theory, we must see to it that the dispersion relations coincide. Using (4.3) and (4.5), we can determine by inversion $\alpha(x)$, (Eringen [1972b], [1974c]). The result is (see also Figure 6)

$$\begin{aligned} \alpha(x) &= \frac{1}{a}\left(1 - \frac{|\underset{\sim}{x}|}{a}\right), \quad \frac{|\underset{\sim}{x}|}{a} \leq 1 \\ &= 0 \qquad\qquad , \quad \frac{|\underset{\sim}{x}|}{a} > 1 \end{aligned} \tag{4.6}$$

Of course, by means of the same considerations for transverse waves, we obtain $\mu'/\mu = \alpha$ so that both $\lambda'(|\underset{\sim}{x}'-\underset{\sim}{x}|)$ and $\mu'(|\underset{\sim}{x}'-\underset{\sim}{x}|)$ are determined.

$$\begin{Bmatrix} \lambda(|x'-x|) \\ \mu(|x'-x|) \end{Bmatrix} = \begin{Bmatrix} \lambda \\ \mu \end{Bmatrix} \alpha(|x'-x|) \tag{4.7}$$

This remarkable result indicates that if the nonlocal moduli vary according to (4.7), the calculations based on the nonlocal theory and the atomic lattice dynamics will be identical.

Note also that the area under the α-curve is unity so that the classical elasticity is obtained when $a \to 0$, i.e., $\alpha(x)$ becomes a Dirac delta measure. For the two- and three-dimensional cases, of course, we have to normalize $\alpha(x)$ by taking the surface or volume integrals of $\alpha(|\underset{\sim}{x}'-\underset{\sim}{x}|)$ over the regions occupied by the body and equate it to unity, i.e.,

$$\int_V \alpha(|\underset{\sim}{x}'-\underset{\sim}{x}|)dv(\underset{\sim}{x}') = 1 \tag{4.8}$$

For the one-dimensional case above this was done by the selection of c_1 as the classical limit.

The foregoing calculations thus determine the nonlocal moduli fully without any unknown parameters so that it must now be tested against other known results. This was done by Eringen [1973b] for Rayleigh surface waves and the dispersion curve found is compared in Figure 7 with the computer calculations of Gazis et al. [1960] based on the atomic lattice dynamics (cf., Maraddudin et al. [1971, p. 531]). The result is unbelievable in that the two curves coincide in the entire Brillouin zone.

Of course, the nonlocal moduli (4.6) are not the only ones that can give us reasonable results. In fact, any non-negative decreasing function with finite support will do just as well. Better yet, one can employ the abundant results from phonon dispersion experiments and by curve fitting obtain a more realistic $\alpha(x)$. Computational problems often force us to select functions that are manageable in calculations. Since we cannot realistically claim that the theory can explain all the physical phenomena associated with few atomic distances, such flexibility is justifiable. Thus, for example, another good function is the Gaussian distribution

$$\alpha(|\underset{\sim}{x}'-\underset{\sim}{x}|) = \alpha_o \exp\left[-\frac{k^2}{a^2}(\underset{\sim}{x}'-\underset{\sim}{x})\cdot(\underset{\sim}{x}'-\underset{\sim}{x})\right] \tag{4.9}$$

where α_o is a constant to be fixed to satisfy (4.8). Here a is the atomic distance and k is a constant. The Fourier transform of (4.9) for the one-dimensional case is shown in Figure 8 for various k. For k=1.65, in fact, this curve coincides with (4.5) in the entire Brillouin zone with an error less than 0.2%. Note, however, that (4.9) will decay fast with $|\underset{\sim}{x}'-\underset{\sim}{x}|$ even if it does not have a finite support. Nevertheless, it goes to a Dirac delta measure as $a \to 0$ so that it is a perfectly suitable nonlocal modulus.

5. CRACK TIP PROBLEM AND FRACTURE MECHANICS

An outstanding example of the difficulty which has been the main cause of the proliferation of fracture theories is the stress singularity predicted by the classical elasticity at a crack tip. A plate with a line crack, subject to uniform tension at infinity perpendicular to the direction of line crack, sustains considerable tension before it starts to tear. Yet classical elasticity predicts an infinite hoop stress at the tip of the crack (Figure 9). Because of this singularity a perfectly good criterion of brittle fracture, the maximum stress hypothesis used for all other types of bodies with no sharp geometrical changes, had to be abandoned. Griffith [1920] discovering this difficulty, said:

> "To explain these discrepancies, but one alternative seemed open. Either the ordinary hypotheses of rupture could be at fault to the extent of 200 or 300 percent, or the method used to compute stresses in the scratches were defective in a like degree."

With his now celebrated work, he gave the criterion for fracture

$$t_o^2 \ell = C_G \quad , \quad C_G \equiv \frac{2E}{\pi(1-\nu^2)} \gamma \tag{5.1}$$

where t_o is the applied tension and ℓ is the half crack length. The Griffith constant C_G is expressed in terms of Young's modulus E, Poisson's ratio ν and the surface tension energy γ. According to (5.1) when the applied stress satisfies (5.1), the crack begins to propagate.

The past half century registered many advances in this field but it can be said that essentially all are influenced by this main idea and the nonexistence of a rational theory that predicts a finite stress at a sharp crack tip. Griffith arrived at this result by using the Inglis [1913] solution of the Elliptic hole problem and letting the excentricity of the ellipse approach zero to obtain a crack. After which he argued that the work done for extending a crack of length 2ℓ by an amount $2d\ell$ must be equal to the surface tension energy. The Griffith criterion may be criticized as follows:

(a) The surface tension energy γ is that of a fluid. For solids there may be other energies arising from surface stresses;

(b) The ellipse shrinking to a crack may not be "uniform," i.e., other shapes may give different limits;

(c) The shear strain at the crack tip is large, namely, $\pi/4$. The crack opens to an ellipse;

(d) Worst of all, the crack tip stress is *infinite* no matter how small the applied load may be.

To remedy some of these defects, Barenblatt [1962], Khristianowich [1955] and Dougdale [1960] introduced compressional cohesive stresses in a small region near the crack tip. By determining the distribution of this superficial stress, Barenblatt closed the tip into a cusp, Figure 10. Kristianowich and Dougdale accomplished the same result by assuming that a constant compressive stress is distributed over an unknown length δ beyond the geometrical tip of the crack so that the tip is closed for a particular value of δ (Figure 11).

Goodier and Kanninen [1966] employed an atomic model with non-linear springs at the edge of the crack and linear springs elsewhere.

Clearly, all these semi-rational and, to some extent, patched-up theories could eliminate some of the objections, nevertheless they replaced the old objections by new ones. For example, how can one conceive of compressive stresses at a free surface unless they are externally applied.

Of course, arguments may also be advanced by insisting that there is no such thing as a sharp crack. The crack tip always has a small radius of curvature even if we produce a crack by removing one line of atoms. Therefore, the singularity is superficial and is the result of a mathematical idealization. While this is true, we have no way of measuring the curvature at the crack tip for these limiting situations. For example, by the removal of one layer of atoms to form a crack do we get positive or negative curvature? What is its magnitude? Since the stress at the crack tip is highly sensitive to the curvature, according to Inglis' solution of elliptic hole problem, in the absence of definitive answers to these questions, no scientific progress is possible.

There exist solutions for the Elliptic hole problem by using polar theories, e.g., couple stress theory (Sternberg and Muki [1967]), micropolar theory (Kim and Eringen [1973]). These solutions also contain the same type of singularities in the limit when the ellipse collapses to a line crack.

Recently, we gave solutions for the problem of a line crack by means of the nonlocal theory, cf., Eringen and Kim [1974a,b], Eringen [1976d], Eringen et al. [1976]. Remarkably, the nonlocal theory not only predicts finite stresses everywhere, but also allows us to unify the fracture criteria in a physically meaningful way. In fact, by use of the maximum stress hypothesis for brittle fracture, we will arrive at the Griffith criterion with the extra benefit that the Griffith constant is now fully determined. As a result of this approach we have been able to calculate the atomic cohesive stresses, which are found to be in excellent agreement with those known from the atomic theory of lattices and experiments. Here we present a brief account of these results.

Introducing the classical Hooke's law

$$\sigma_{k\ell}(\underset{\sim}{x}') \equiv \sigma'_{k\ell} = \lambda e'_{rr}(\underset{\sim}{x}')\delta_{k\ell} + 2\mu e'_{k\ell}(\underset{\sim}{x}') \tag{5.2}$$

We write $(3.9)_1$ as

$$t_{k\ell} = \int_V \alpha(|\underset{\sim}{x}'-\underset{\sim}{x}|)\sigma_{k\ell}(\underset{\sim}{x}')dv(\underset{\sim}{x}') \tag{5.3}$$

Substituting this into Cauchy's equations (2.7), with $\hat{\rho}=0$, $\hat{f}=0$ in the static case, we obtain

$$\int_V \alpha(|\underset{\sim}{x}'-\underset{\sim}{x}|)\sigma_{\kappa\ell,k'}(\underset{\sim}{x}')dv(\underset{\sim}{x}') - \int_{\partial V} \alpha(|\underset{\sim}{x}'-\underset{\sim}{x}|)\sigma_{k\ell}(\underset{\sim}{x}')dv(\underset{\sim}{x}') = 0 \qquad (5.4)$$

where we used the Green-Gauss theorem (in absence of σ). When the body extends to infinity in all directions or the surface tensions are negligible, the surface integral in (5.4) vanishes and we have

$$\int_V \alpha(|\underset{\sim}{x}'-\underset{\sim}{x}|)\sigma_{k\ell,k'}(\underset{\sim}{x}')dv(\underset{\sim}{x}') = 0 \qquad (5.5)$$

It can be proven that, cf., Eringen [1976e], when $\alpha(|\underset{\sim}{x}'|)$ is a continuous function of $\underset{\sim}{x}'$ with a bounded support where $\alpha>0$, (5.5) is satisfied if and only if

$$\sigma_{k\ell,k} = 0 \qquad (5.6)$$

Using (5.2), this gives the classical Navier's equations. For the two-dimensional case the solution of Navier's equations for the displacement fields are, (cf., Sneddon [1951, p. 404]):

$$u(x,y) = \frac{1}{\sqrt{2\pi}} \int_{-\infty}^{\infty} \frac{1}{k}\left[|k|A(k) + \left(|k|y - \frac{\lambda+3\mu}{\lambda+\mu}\right)B(k)\right] \exp(-|k|y-ikx)dk,$$

$$v(x,y) = \frac{1}{\sqrt{2\pi}} \int_{-\infty}^{\infty} [A(k) + yB(k)] \exp(-|k|y-ikx)dk \qquad (5.7)$$

where A(k) and B(k) are two functions to be determined from the boundary conditions (see Figure 12).

$$\begin{aligned} t_{yx} &= 0 \quad , \quad y = 0 \quad , \quad \forall x \\ t_{yy} &= -t_o \quad , \quad y = 0 \quad , \quad |x| < \ell \\ v &= 0 \quad , \quad y = 0 \quad , \quad |x| > \ell \end{aligned} \qquad (5.8)$$

Using $(5.8)_1$ we express B in terms of A and the remaining two conditions lead to a pair of dual integral equations which must be solved to determine A(k). These equations are *non-singular*. We have reduced them to a single Fredholm equation of the second kind and solved it numerically (see Eringen et al. [1976]). By superimposing t_o to the stress field, we obtained the solution of the crack problem, in which the crack surface is free of tractions but at $y=\infty$ a uniform tension t_o stretches the plate.

The Hoop stress distribution along the crack line is shown in Figures 13 and 14. It is clear from these figures that the stress t_{yy} has a maximum at the crack tip thereafter diminishing smoothly to the classical elasticity solution. Important to the fracture mechanics is the maximum stress (or the stress concentration) which is given by

$$P = t_{yy}(\ell,0)/t_o = C(\nu)(2\ell/a)^{\frac{1}{2}} \tag{5.9}$$

The function $C(\nu)$ depends on Poisson's ratio ν only and it falls into the region $0.676 \leq C(\nu) \leq 0.845$ for $\nu=0$ to 0.5, see Figure 15. For $\nu=0.25$, $C=0.713$. We observe:

(i) The hoop stress (for that matter all stress components) is *finite* as long as $a \neq 0$ (a=atomic distance). In the continuum limit $a \to 0$, the classical square root singularity appears.

(ii) By equating the maximum stress to the failure stress, we establish a failure criterion. In fact, we state that: *when* $t_{yy\,max} = t_c$ = *cohesive stress, fracture will occur.*

This most natural criterion is not only physical in nature because of attributing the fracture to bond failure but it also agrees with the engineering failure criterion commonly used in structural mechanics. This has only been possible since the nonlocal theory removes the stress singularity at the crack tip.

From (5.9) it now follows that

$$t_o^2 \ell = [a/2\ C^2(\nu)]\ t_c^2 \equiv C_G \tag{5.10}$$

Alas, this is the Griffith fracture criterion for brittle fracture with the extra benefit that C_G is now fully determined. No *ad hoc* constant such as surface energy γ appears in (5.10);

(iii) It is clear that C_G is a material property. This seemingly simple and obvious result has been under extensive experimental investigations until recently. In fact, engineering fracture toughness defined by $K_I = \sqrt{\pi\ell}\ t_o = (\pi C_G)^{\frac{1}{2}}$ was tested extensively (cf., Freed et al. [1971]; Brown and Strawley [1966].

(iv) Experimenters also determined the surface tension energy by one means or another for various materials. While the accuracy of such experiments are often questioned if we equate C_G given by (5.10) to the Griffith expression $(5.1)_2$, we obtain

$$t_c^2 a = K\gamma \qquad , \qquad K \equiv 8C^2(\nu)\mu/\pi(1-\nu) \tag{5.11}$$

Calculations may now be carried out to determine the cohesive stress for various materials. This was done by Eringen [1976d] and the results are listed in the column next to the last in Table 1. The entries in the last column of this table are estimates of t_c/E based on atomic considerations, see Lawn & Wilshaw [1975, p. 160]. The remarkably close values obtained are once again indicative of the far-reaching power of the nonlocal theory.

6. SCREW DISLOCATION

A screw dislocation is obtained if the lower face of a radial plane of a cylinder is given a constant relative displacement b, in the direction of the axis of the cylinder with respect to its upper face, Figure 17. Here b is known as the *Burgers vector*. Employing cylindrical coordinates, $r,\theta,z,$, the classical elasticity solution of this problem may be expressed as (cf., Lardner [1974, p. 72]).

$$u_z = \frac{b\theta}{2\pi} \quad , \quad u_r = u_\theta = 0 \tag{6.1}$$

where (u_r,u_θ,u_z) denote the components of the displacement vector in cylindrical coordinates. For the local stress field, $\sigma_{k\ell}$ we have

$$\sigma_{z\theta} = \frac{\mu b}{2\pi r} \quad , \quad \text{all other } \sigma_{k\ell} = 0 \tag{6.2}$$

so that any cylindrical surface $r=R$ is free of traction. The solutions (6.1) and (6.2) are also the solutions of the problem in nonlocal elasticity (cf., 5.6). However, to calculate the stress field in nonlocal elasticity, we must perform the volume integration in (5.3). Employing (4.9) for $\alpha(|\underset{\sim}{x}'-\underset{\sim}{x}|)$, calculations were carried out (cf., Eringen [1976e]). The result is

$$t_{z\theta} = \frac{\mu b}{2\pi r} \left[1 - \exp(-k^2r^2/a^2)\right] \quad , \quad \text{all other } t_{k\ell} = 0 \tag{6.3}$$

We have also carried out calculations for the strain energy function Σ given by $(3.9)_2$

$$\Sigma = \frac{\mu b^2 L}{8\pi} \left[C + \ell n(P^2) - Ei(-P^2)\right] \quad , \quad P \equiv kR/a \tag{6.4}$$

TABLE 1. Cohesive Stress. t_c: $t_c^2 a = K\gamma$

$K \equiv 8C^2\mu/\pi(1-\nu)$

a = Atomic dist.

γ = Surface energy

Experimental[1]						Present Theory					Atomistic Models[2]
Type	Crystal	γ CGS	$\mu x10^{-11}$ CGS	ν	a A^o	C(ν)	$Kx10^{-11}$ CGS	$K\gamma$ x 10^{-14}	t_c x 10^{-11}	t_c/E	t_c/E
Face C.	Al	840	2.51	0.347	2.86	0.743	5.402	4.538	1.260	0.186	
	Ni	1725	7.48	0.276	2.49	0.719	13.57	23.41	3.066	0.16	
Body C.	Fe	1975	6.92	0.291	2.48	0.721	12.93	25.53	3.209	0.18	0.23
Ionic	LiF	380	4.40	0.068	2.014	0.684	5.621	2.698	1.157	0.123	
Diam.	C	5400	50.9	0.187	1.54	0.701	78.32	422.9	16.57	0.137	0.17
Hex.	Zn	575	3.83	0.333	2.66	0.736	7.925	4.557	1.309	0.128	0.11

[1] γ, μ and ν are taken from data collected by Rice and Thomson [1974, Table 1]. Lattice parameter a is from Kittel [1971, Table 5].

[2] Atomistic results are from Table 7.1, p. 160, Lawn and Wilshaw [1975].

where R is the outer radius of the cylinder, C is the Euler's constant and Ei(x) is the exponential integral function,

$$C = 0.577216\ldots\ ; \qquad Ei(-x) = -\int_x^\infty \frac{e^{-t}}{t}\,dt \quad , \quad x>0 \tag{6.5}$$

The solution of this problem in classical elasticity is given by

$$t_{z\theta} = \frac{\mu b}{2\pi r} \tag{6.6}$$

$$\Sigma = \frac{\mu b^2}{4\pi}\,\ell n(R/r_o) \tag{6.7}$$

where L is the length of the cylinder. In classical elasticity, not only the stress is singular at $r=0$ but also the stored elastic energy. For that reason we are forced to consider the solution valid only in a hollow cylinder with inner radius r_o. While the stress singularities are common in elasticity, the energy singularity is certainly a strange phenomena that cannot be tolerated.

The nonlocal elasticity solution of this problem predicts a shear stress with no singularity (cf., Eq. 6.3). The stored energy is not singular either (see Eq. 6.4). In the classical limit as $a \to 0$ both (6.3) and (6.4) reduce to the classical results (6.6) and (6.7).

Because of the singularities present in the classical solutions, solid state physicists have invented various atomic devices and terminology to overcome this difficulty. The semi-continuum model of Peirls [1940] and Nabarro [1947] are two such examples. It must be remarked that in the classical solution $t_{z\theta} \to \infty$ as $r \to 0$ at $\theta=0$, $t_{z\theta} \to -\infty$ as $r \to 0$ $\theta=2\pi$. Clearly, the physical considerations demand that $t_{z\theta}$ must be skew-symmetric with respect to x and thus must vanish at $r=0$. Indeed, this is born out by the nonlocal solution $t_{z\theta}=0$ at $r=0$, Figure 17. However, it possesses a maximum at the root $\rho=\rho_m$ of

$$\exp(\rho^2) = 1 + 2\rho^2 \quad , \quad \rho \equiv kr/a \tag{6.8}$$

The maximum shear stress is

$$t_{z\theta\,max} = \frac{\mu b k}{\pi a}\ \rho_m(1 + 2\rho_m^2)^{-1} \tag{6.9}$$

We now obtain a very important result for failure. In fact, it is natural to assume that the failure occurs when $t_{z\theta\,max}$ is equal to the *cohesive*

shear stress τ_c . We can calculate the critical shear to cause a dislocation, having a Burger's vector b. From (7.8) this is obtained to be

$$\tau_c = 0.3191 \frac{\mu b k}{\pi a} \tag{6.10}$$

We may estimate the value of k from the rate of attenuation of interatomic forces. For example, for k=1.073 the interatomic forces will reduce to 1 percent of their values at two-atomic distances. This value is also close to the value estimated by the dispersion of one-dimensional waves (cf., Figure 8). Using k=1.073 we can calculate the stress that will just overcome the cohesive shear stress necessary to create a dislocation of one atomic distance. For face-centered cubic metals $b=a/\sqrt{6}$ and we obtain

$$\tau_c/\mu = 0.0345 \tag{6.11}$$

For aluminum, the tabulated value is $\tau_c/\mu=0.039$ and for copper at 20°C, $\tau_c/\mu=0.039$ (Kelly [1966, p. 19]).

The problem of edge dislocation has also been treated (Eringen [1966f]). While the problem is somewhat more complicated, the results are are again extremely gratifying. Excellent agreements obtained with the atomic lattice dynamics and experiments once again point to the great potential of the nonlocal continuum theory.

7. SECONDARY FLOW IN RECTANGULAR PIPES

The theory of nonlocal fluid mechanics has already been developed in our previous work (cf., Eringen [1972c], [1976a]). Here we discuss, briefly, some very significant results in the development of vortices in a rectangular channel.

A viscous fluid contained in a long rectangular pipe, initially at rest, is set into motion by an impulsively applied, and maintanined uniform pressure gradient, Figure 18. The velocity profile predicted by the Navier-Stokes theory is unidirectional $v_x=v_y=0$ $v_z=v(x,y,t)$, as shown in Figure 19 for 2x1 pipe. Experiments show that this type of flow is unstable. When the Reynolds' number exceeds a certain critical value (based on the mean velocity and hydraulic diameter, 2000), secondary flow sets in and the flow regime becomes turbulent. The Navier-Stokes theory contains no direct mechanism for the creation of secondary flow. Although some higher order rate-dependent fluids (e.g., Reiner-Rivlin) have been employed to explain the secondary flow patterns, the applicability

of these models and the physical basis of the secondary flow mechanisms in these theories have been questioned. The structure of secondary flow in a 2x1 rectangular pipe, as observed experimentally, is shown in Figure 20. It is known that the vortices of the secondary flow emanate from the corners of the pipe. For the nucleation of the flow, it is reasonable to assume that an internal friction mechanism on the atomic or molecular scale is necessary. This means again, a long range intermolecular effect which is lacking in all previously known fluid flow theories.

The nonlocal fluid dynamics was developed in our work [1972c]. Since turbulent stresses are nonlinear in character, we have recently extended this theory to include second degree nonlinear effects in the constitutive equations. For an incompressible fluid, the stress constitutive equation was found to be of the form

$$t_{k\ell} = -p\delta_{k\ell} + 2\mu d_{k\ell} + \int_V \mu'(|\underset{\sim}{x}'-\underset{\sim}{x}|)\{(x'_k-x_k)[d_{\ell m}(\underset{\sim}{x}')-d_{\ell m}(\underset{\sim}{x})]\beta_m(\underset{\sim}{x}')$$

$$+ (x'_\ell-x_\ell)[d_{km}(\underset{\sim}{x}') - d_{km}(\underset{\sim}{x})]\beta_m(\underset{\sim}{x}')\}d\upsilon(\underset{\sim}{x}') \qquad (7.1)$$

where $d_{k\ell}$ is the deformation rate tensor, $p(\underset{\sim}{x},t)$ is the pressure, $\mu'(|\underset{\sim}{x}'-\underset{\sim}{x}|)$ is the nonlocal viscosity modulus and $\beta_k(\underset{\sim}{x}')$ is an objective measure of relative motion (not present in classical theories, cf., Eringen [1972c])

$$d_{k\ell} = \tfrac{1}{2}(v_{k,\ell} + v_{\ell,k}) \quad , \quad d_{k\ell}(\underset{\sim}{x}') = \tfrac{1}{2}(v'_{k,\ell} + v'_{\ell,k})$$

$$\beta_k(\underset{\sim}{x}') = \tfrac{1}{2}(x'_m-x_m)[v_{m,k}(\underset{\sim}{x}') - v_{m,k}(\underset{\sim}{x})] + v_k(\underset{\sim}{x}') - v_k(\underset{\sim}{x}) \qquad (7.2)$$

Here $\underset{\sim}{x}$ is a spatial point at which $t_{k\ell}$ is evaluated; $\underset{\sim}{x}'$ is any other point, and $\underset{\sim}{v}(\underset{\sim}{x})$ and $\underset{\sim}{v}(\underset{\sim}{x}')$ are the velocity fields at $\underset{\sim}{x}$ and $\underset{\sim}{x}'$ respectively. It must be noted that (7.1) does not violate the second law of thermodynamics, i.e.,

$$\int_V \frac{1}{\theta}\,(t_{k\ell} + p\delta_{k\ell})d_{k\ell}\,d\upsilon \geq 0$$

is satisfied for all possible motions. In fact, (7.1) is not only justifiable on physical grounds (such as objectivity, thermodynamic admissibility) but turns out to be in accordance with a representation theorem on additive functionals due to Frideman and Katz [1965] although

we were not aware of the existence of this theorem at the time of the publication of our theory.

Employing (7.1) in Cauchy's equations of motion (2.7) with $\hat{\rho}=0$ $\hat{\underset{\sim}{f}}=\underset{\sim}{0}$, we obtain three integro-partial differential equations for $\underset{\sim}{v}$ and p. Together with the continuity equation div $\underset{\sim}{v}=0$, this set is adequate for the determination of the velocity field. We have carried out these calculations to determine the velocity field in a long rectangular pipe.

$$\underset{\sim}{v} = \{ u(x,y,t) \quad , \quad v(x,y,t) \quad , \quad w(x,y,t) \}$$

For the nonlocal modulus μ' we have selected

$$\mu'(|\underset{\sim}{x}'-\underset{\sim}{x}|) = \mu_o \exp(-k_o|\underset{\sim}{x}-\underset{\sim}{x}'|)$$

where μ_o and k_o are constants. In general, k_o can be chosen so that $\mu'(|\underset{\sim}{x}'-\underset{\sim}{x}|)$ attenuates properly over a characteristic length of the problem (e.g., a mixing length). μ_o is a normalization factor that was chosen to produce a proper relative size for the secondary flow with respect to the mean flow. This constant is unimportant as far as the mechanism of the secondary flow is concerned.

By means of a finite difference technique, computer calculations were carried out for a 2x1 pipe. The streamlines of the secondary flow at various times are shown in Figures 21-25. The pressure gradient was selected to yield a Reynolds number of approximately 2500 which is in the transition region to turbulence. Small eddies form at the corners (Figure 21) and then gradually diffuse to the interior of the pipe. The steady state solution (Figure 25) is in remarkable agreement with experimental results shown in Figure 26. The lines of constant velocity emanating from corners (dotted lines in Figure 26) are 45° lines due to the symmetry of the problem. Computed lines of constant velocity (Figure 25) are also approximately 45°. Experimentally available secondary flow profiles for a Reynolds number 50,000 are shown in Figure 26. These profiles are relatively flat at the pipe wall because of high Reynolds numbers. The secondary flow profiles (Re=2500) predicted by the nonlocal theory are shown in Figure 27. The comparison of profiles are favorable even though Reynold's numbers are substantially different.

Clearly, much remains to be investigated for more conclusive judgments on the theory of nonlocal fluid mechanics. This example is

shown in order to induce adequate curiosity and appetite to learn and apply the theory to many important problems in turbulence that have remained in an *ad hoc* and heuristic stage for a long time.

8. PROSPECTS

With this rather brief account, I have tried to present some of our recent research efforts in the field of nonlocal continuum mechanics. Examples of solutions are presently too few on account of the fact that the theory is only a few years old. It is yet to be more fully challenged and tested on other critical grounds. While we are, substantially, in possession of the solutions of several other problems (e.g., punch problem, surface tension and E-M wave propagations) I believe for this lecture, the solutions presented bring to focus the power and potential of the theory. The theory cannot be accused of having a large number of parameters for the purpose of curve-fitting. Once the nonlocal moduli are determined by means of some simple atomic or molecular considerations (or experiments) the theory is fully determinate for a given material. From the foregoing acid tests, it is clear that we can discuss the nature of physical phenomena on the atomic scale. Since the theory is a continuum theory, in principle, every problem is reducible to a boundary-initial value problem which is often not possible in the atomic theories on account of the free surface conditions and complicated inner structure. The surface physics is also incorporated into the theory, which is an unusual asset yet to be tapped.

Acknowledgment

I am indebted to Mr. Charles Speziale for carrying out computer calculations on the pipe flow problem and checking part of the analysis.

References

Barenblatt, G.E. [1962] "The Mathematical Theory of Equilibrium Cracks in Brittle Fracture," Advan. Appl. Mech., 7, pp. 55-129.

Brillouin, L. [1953] Wave Propagation in Periodic Structures, Dover, p. 4.

Brown, W.F. and Strawley, J.E. [1966] "Plane Strain Crack Toughness Testing of High Strength Metallic Materials," ASTM Special Technical Publication No. 410, p. 20.

Dugdale, D.S. [1960] "Yielding of Steel Sheets Containing Slits," J. Mech. Phys. of Solids, 8, pp. 100-104.

Eringen, A.C. [1967] Mechanics of Continua, New York: John Wiley & Sons, 502 pp.

Eringen, A.C. [1972a] "Nonlocal Polar Elastic Continua," Int. J. Engng. Sci., 10, pp. 1-16.

Eringen, A.C. [1972b] "Linear Theory of Nonlocal Elasticity and Dispersion of Plane Waves," Int. J. Engng. Sci., 10, pp. 425-435.

Eringen, A.C. [1972c] "On Nonlocal Fluid Mechanics," Int. J. Engng. Sci., 10, pp. 561-575.

Eringen, A.C. [1973a] "Theory of Nonlocal Electromagnetic Elastic Solids," J. Math. Phys., 14, pp. 733-740.

Eringen, A.C. [1973b] "On Rayleigh Surface Waves with Small Wave Length," Lett. Appl. & Engng. Sci., 1, pp. 11-17.

Eringen, A.C. [1974a] "On Nonlocal Continuum Thermodynamics," Modern Developments in Thermodynamics, (ed. B. Gal-Or), New York: John Wiley & Sons, pp. 121-142.

Eringen, A.C. [1974b] "Theroy of Nonlocal Thermoelasticity," Int. J. Engng. Sci., 12, pp. 1063-1077.

Eringen, A.C. [1974c] "Nonlocal Elasticity and Waves," Continuum Mechanics Aspects of Geodynamics and Rock Fracture Mechanics, (ed. P. Thoft-Christensen), Dordrecht, Holland: D. Reidel Publishing Co., pp. 81-105.

Eringen, A.C. [1976a] "Nonlocal Polar Field Theories," Continuum Physics, Vol. 4 (ed. A.C. Eringen), New York: Academic Press, pp. 205-267.

Eringen, A.C. [1976b] "Polar and Nonlocal Theories of Continua and Applications," Bogazici University Publications - 75-35/01 (20 lectures given at Bogazici University, Turkey).

Eringen, A.C. [1976c] "On Bridging the Gap Between Macroscopic and Microscopic Physics," Recent Advances in Engineering Science, 6.

Eringen, A.C. [1976d] "State of Stress in the Neighborhood of a Sharp Crack Tip, Princeton Technical Report No. 43.

Eringen, A.C. [1976e] "Screw Dislocation in Nonlocal Elasticity," Princeton Technical Report No. 41, accepted for publication in J. of Physics D: Applied Physics.

Eringen, A.C. [1976f] "Edge Dislcoation in Nonlocal Elasticity," Princeton Technical Report No. 42.

Eringen, A.C. and Edelen, D.G.B. [1972] "On Nonlocal Elasticity," Int. J. Engng. Sci., 10, pp. 233-248.

Eringen, A.C. and Kim, B.S. [1974a] "On the Problem of Crack Tip in Nonlocal Elasticity," Continuum Mechanics Aspects of Geodynamics and Rock Fracture, (ed. P. Thoft-Christensen) Dordrecht, Holland: D. Reidel Publishing Co., pp. 107-113.

Eringen, A.C. and Kim, B.S. [1974b] "Stress Concentration at the Tip of Crack," Mech. Res. Comm., 1, pp. 233-237.

Eringen, A.C., Speziale, C.G. and Kim, B.S. [1976] "Crack Tip Problem in Nonlocal Elasticity," Princeton Technical Report No. 44.

Freed, C.N., Sullivan, A.M. and Stoop, J. [1971] "Influence of Dimensions of Center-Cracked Tension Specimen on K_C," ASTM Special Technical Publication No. 514, p. 109.

Friedman, N. and Katz, M. [1966] "A Representation Theorem for Additive Functionals," Arch. Rat. Mech. Anal., Vol. 21, pp. 49-57.

Gazis, C.D., Herman, R. and Willis, R.F. [1960] Phys. Rev., 119, p. 533.

Gessner, F.B. and Jones, J.B. [1965] "On Some Aspects of Fully-Developed Turbulent Flow in Rectangular Channels," J. Fluid Mech., 23, 689.

Goodier, J.N. and Kanninen, M. [1966] "Crack Propagation in a Continuum Model with Nonlinear Atomic Separation Laws," Technical Report No. 165 (Contract under the Office of Naval Research) Division of Engineering Mechanics, Stanford, University.

Griffith, A.A. [1920] "The Phenomena of Rupture and Flow in Solids," Phil. Trans. Roy. Soc. (London), Ser. A221, pp. 163-198.

Inglis, C.E. [1913] "Stresses in a Plate Due to the Presence of Cracks and Sharp Corners," Proc. Inst. Naval Architects.

Kelly, A. [1966] Strong Solids, Oxford: Clarendon Press.

Kim, B.S. and Eringen, A.C. [1973] "Stress Distribution Around an Elliptic Hole in an Infinite Micropolar Elastic Plate," Lett. Appl. & Engng. Sci., 1, pp. 381-390.

Kröner, E [1967] "Elasticity Theory with Long Range Cohesive Forces," Int. J. Solids Struct., 3, p. 731.

Krumhansl, J.A. [1965] "Generalized Continuum Field Representations for Lattice Vibrations," Lattice Dynamics (R.F. Wallis, ed.) Pergamon, Oxford.

Krumhansl, J.A. [1968] "Some Considerations on the Relations Between Solid State Physics and Generalized Continuum Mechanics," Mechanics of Generalized Continua, (E. Kroner, ed.) Springer-Verlag, Berlin.

Kunin, I.A. [1966a] "Model of Elastic Medium with Simple Structure and Space Dispersion," (in Russian), Prikl. Mat. Mekh., 30, p. 542.

Kunin, I.A. [1966b] "Theory of Elasticity with Space Dispersion. One-Dimensional Continuum Structure," Prikl. Mat. Mekh., 30, 866.

Kunin, I.A. [1967a] "The Theory of Elastic Media with Microstructure and the Theory of Dislocations," Mechanics of Generalized Continua (E. Kroner, ed.) Springer-Verlag, Berlin.

Kunin, I.A. [1967b] "Internal Stresses in Media with Microstructure," Prikl. Mat. Mech., 21, p. 889.

Kunin, I.A. [1968] "Theories of Elastic Media with Microstructure," Proc. Vibr. Probl., 9, 323.

Lawn, B.R. and Wilshaw, T.R. [1975] Fracture of Brittle Solids, Cambridge University Press (London).

Lardner, R.W. [1974] Mathematical Theory of Dislocations and Fracture, University of Toronto Press.

Maraddudin, A.A., Montroll, E.W., Weiss, G.H. and Ipatova, I.P. [1971] Theory of Lattice Dynamics in the Harmonic Approximation, Second edition, Academic Press, p. 531.

Nabarro, F.R.N. [1947] "Dislocations in a Simple Cubic Lattice," Proc. Roy. Soc., 59, pp. 256-272.

Peirls, R.E. [1940] "The Size of a Dislocation," Proc. Roy. Soc., 52, pp. 34-37.

Rogula, D. [1965] "Influence of Spatial Acoustic Dispersion on Dynamical Properties of Dislocations, I., Bull. Acad. Pol. Sci., Sci. Techn., 13, p. 337.

Sneddon, I.N. [1951] Fourier Transform, McGraw-Hill Book Co., New York.

Sternberg, E. and Muki, R. [1967] "The Effect of Couple Stresses on the Stress Concentration around a Crack," Int. J. Solids & Structures, 3, p. 69.

Zheltov, Iu, P. and Khristianovich, S.A. [1955] Izv. Acad. Nauk SSSR Otd Teckn. Nauk, 5, pp. 3-41.

Figure Captions

Figure 1. Moving Discontinuity Surface σ

Figure 2. Dispersion Relations for Copper, after Sinha & Squires [1963]

Figure 3. Experimental dispersion curves for phonons propagating in the [100] direction in aluminum. For this direction of propagation, the reduced wave number is given by $\zeta = (a/2\pi)|q|$, where q is the phonon wave vector, and a is the lattice constant of aluminum. The error in ω is estimated to be in the range 1-2 percent. After Yarnel et al. [1973].

Figure 4. Infinite Lattice with the Nearest Interactions (Born vonKármán model)

Figure 5. Dispersion Relations (1 Brillouin Zone)

Figure 6. Nonlocal Elastic Moduli

Figure 7. Dispersion of Surface Waves

Figure 8. Dispersion Curves Based on Gaussian Type Nonlocal Moduli

Figure 9. Hoop Stress Along Crack Line (classical elasticity)

Figure 10. Barenblatt's Hypothesis

Figure 11. Khristianowich-Dougdale Hypothesis

Figure 12. Crack Problem

Figure 13. Hoop Stress Distribution Along Crack Line $P = t_{yy}/t_o$

Figure 14. Hoop Stress Distribution Along Crack Line $P \equiv t_{yy}/t_o$

Figure 15. Material Function $C(\nu)$

Figure 16. Screw Dislocation

Figure 17. Shear Stress in Screw Dislocation

Figure 18. Flow in Rectangular Pipe Induced by an Impulsively Applied Pressure Gradient -G

Figure 19. Velocity Profiles at Centerline of 2x1 Rectangular Pipe from Navier-Stokes Theory (obtained numerically)

Figure 20. Experimental Secondary Flow Velocity Profiles at Various Stations Along the x-axis in 2x1 Rectangular Pipe After Gessner and Jones [1965]

Figure 21. Secondary Flow Pattern in 2x1 Rectangular Pipe Obtained from the Nonlocal Fluid Mechanics. RE ≈ 2500, $\mu_o/\rho = -10^6$ ft^{-2}, $k_o = 1000$ ft^{-1}

Figure 22. Secondary Flow Pattern in 2x1 Rectangular Pipe Obtained from the Nonlocal Fluid Mechanics. RE ≈ 2500, $\mu_o/\rho = -10^6$ ft^{-2}, $k_o = 1000$ ft^{-1}

Figure 23. Secondary Flow Pattern in 2x1 Rectangular Pipe Obtained from the Nonlocal Fluid Mechanics. RE ≈ 2500, $\mu_o/\rho = -10^6$ ft^{-2}, $k_o = 1000$ ft^{-1}

Figure 24. Secondary Flow Pattern in 2x1 Rectangular Pipe Obtained from the Nonlocal Fluid Mechanics. RE ≈ 2500, $\mu_o/\rho = -10^6$ ft^{-2}, $k_o = 1000$ ft^{-1}

Figure 25. Secondary Flow Pattern in 2x1 Rectangular Pipe Obtained from the Nonlocal Fluid Mechanics

Figure 26. Secondary Flow Pattern at Various Stations Along the x-axis in 2x1 Rectangular Pipe Obtained from the Nonlocal Fluid Mechanics

Figure 27. Secondary Flow Velocity Profiles at Various Stations Along the x-axis in 2x1 Rectangular Pipe Obtained from the Nonlocal Theory

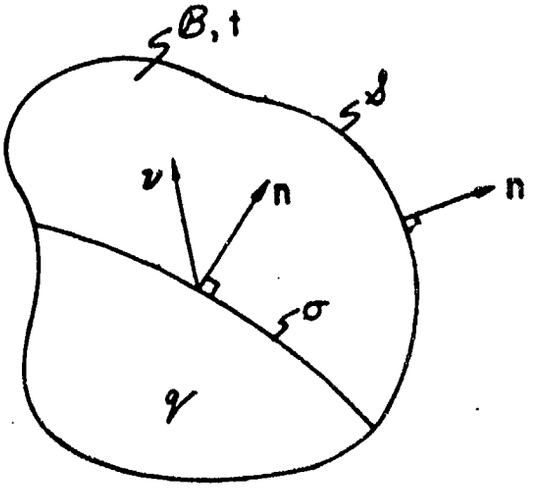

Figure 1

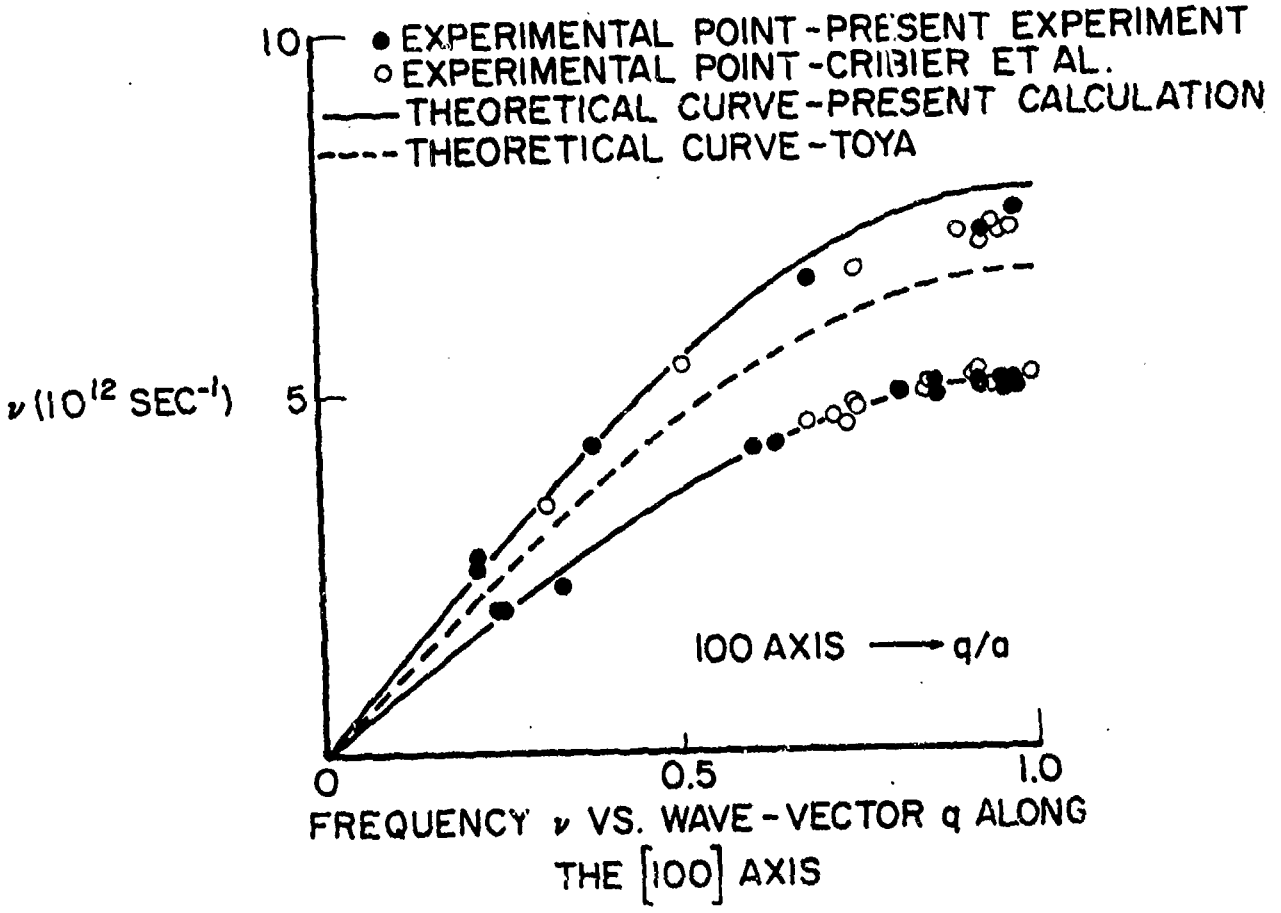

FREQUENCY ν VS. WAVE-VECTOR q ALONG THE [100] AXIS

Figure 2

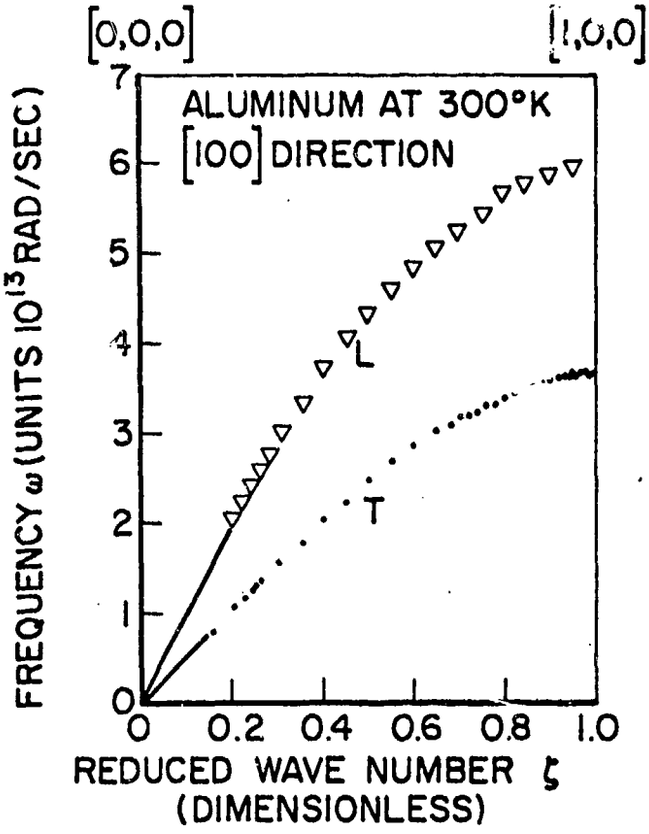
[0,0,0]
[1,0,0]
ALUMINUM AT 300°K
[100] DIRECTION
L
T
FREQUENCY ω (UNITS 10^13 RAD/SEC)
0
1
2
3
4
5
6
7
0
0.2
0.4
0.6
0.8
1.0
REDUCED WAVE NUMBER ζ
(DIMENSIONLESS)

Figure 3

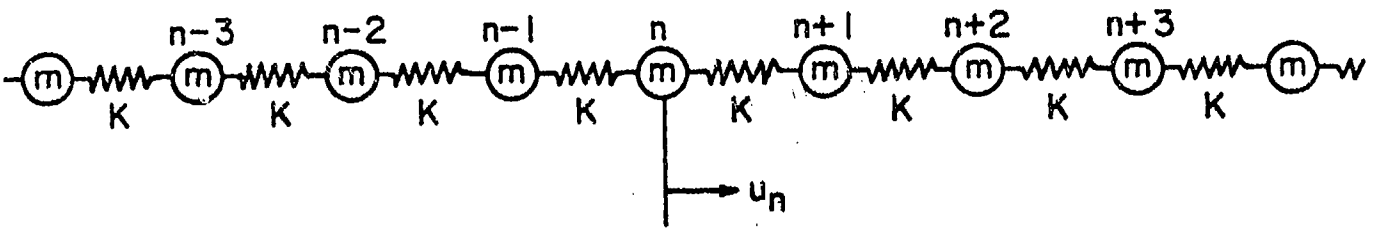

Figure 4

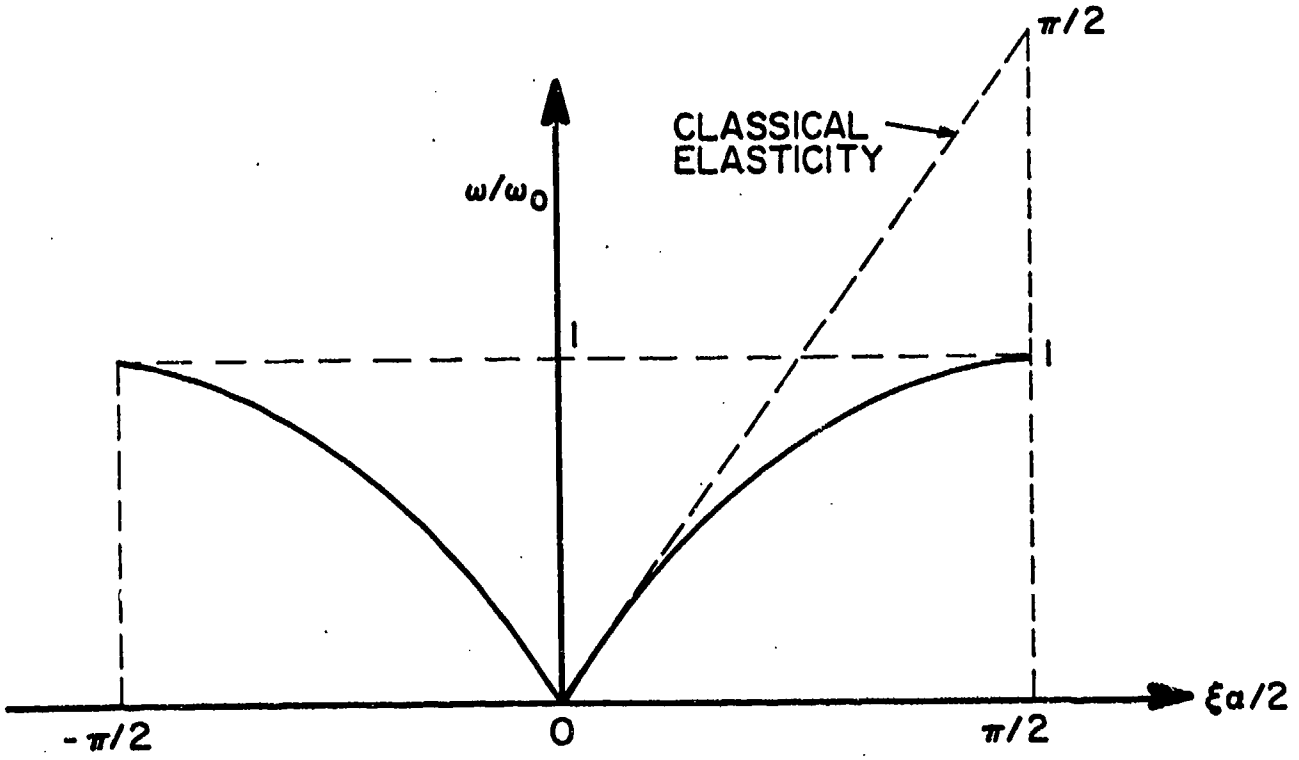

Figure 5

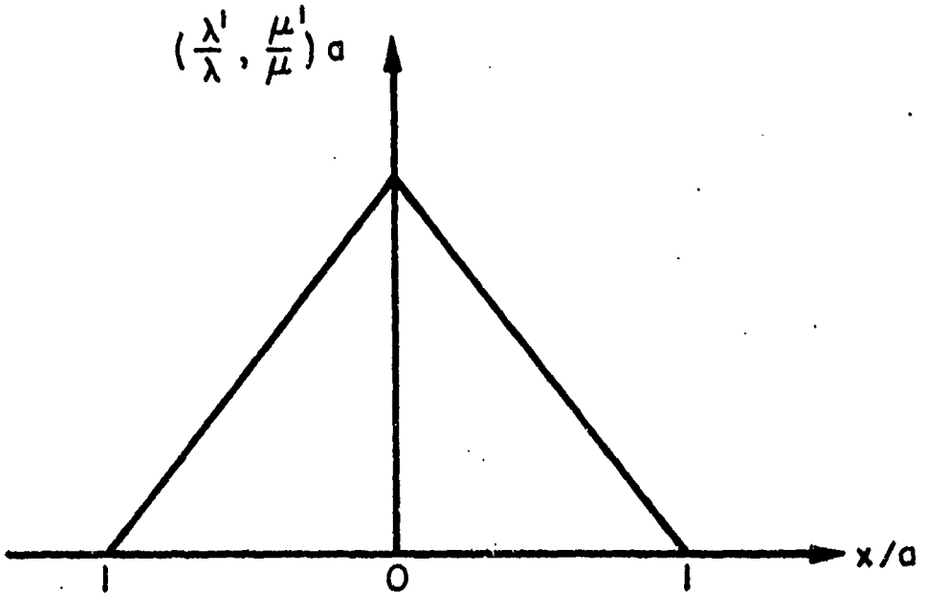

Figure 6

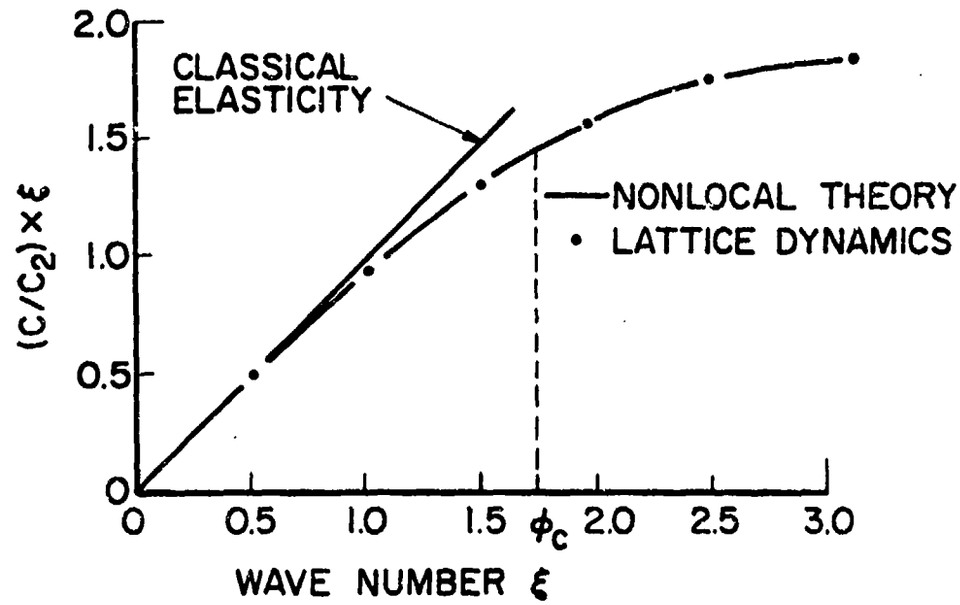
2.0
1.5
1.0
0.5
0
$(C/C_2) \times \xi$
CLASSICAL
ELASTICITY
NONLOCAL THEORY
LATTICE DYNAMICS
0
0.5
1.0
1.5
ϕ_c
2.0
2.5
3.0
WAVE NUMBER ξ

Figure 7

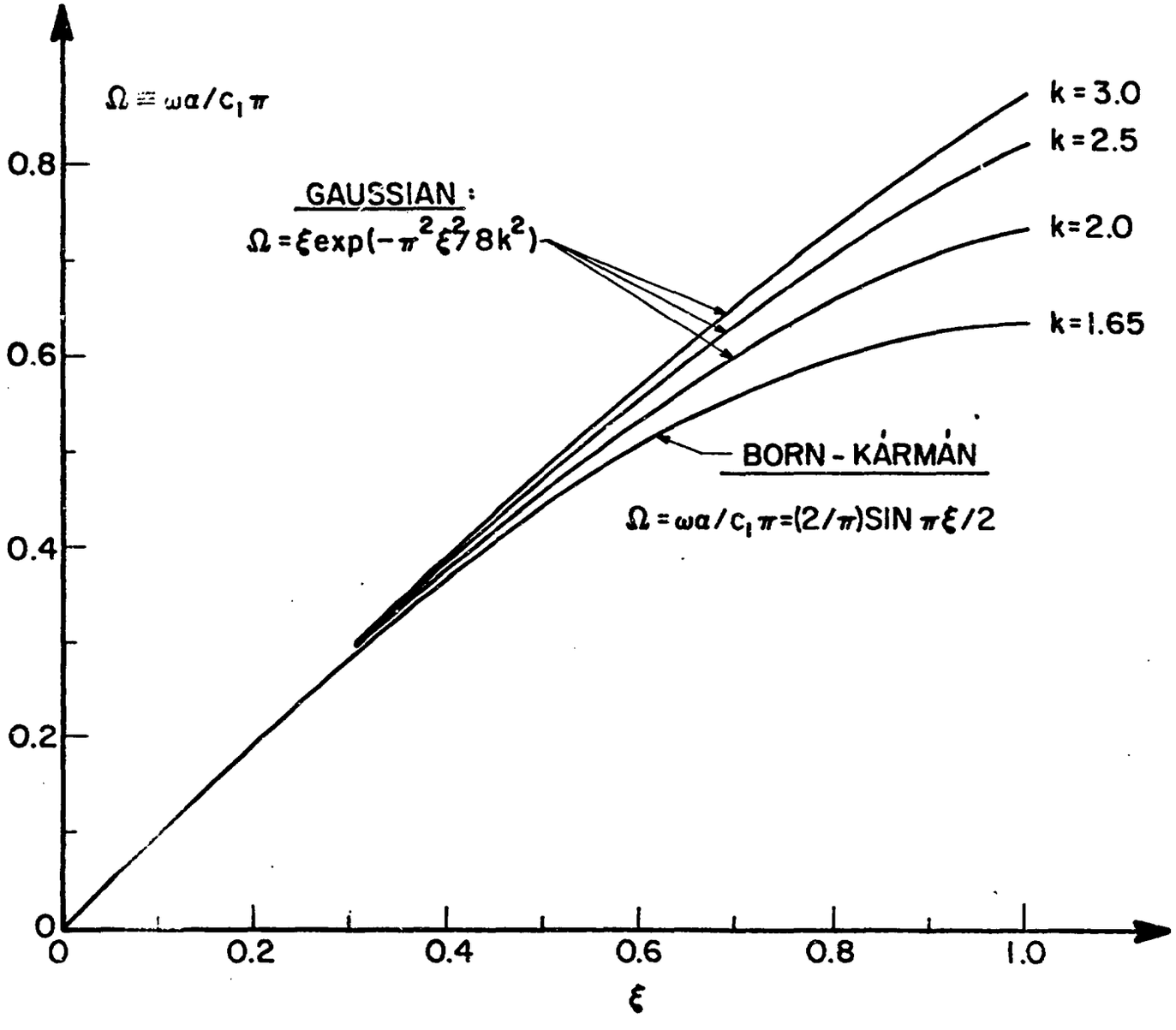
Ω ≡ ωa/c₁π
0.8
0.6
0.4
0.2
0
GAUSSIAN :
Ω = ξexp(−π²ξ²/8k²)
k = 3.0
k = 2.5
k = 2.0
k = 1.65
BORN - KÁRMÁN
Ω = ωa/c₁π = (2/π)SIN πξ/2
0
0.2
0.4
0.6
0.8
1.0
ξ

Figure 8

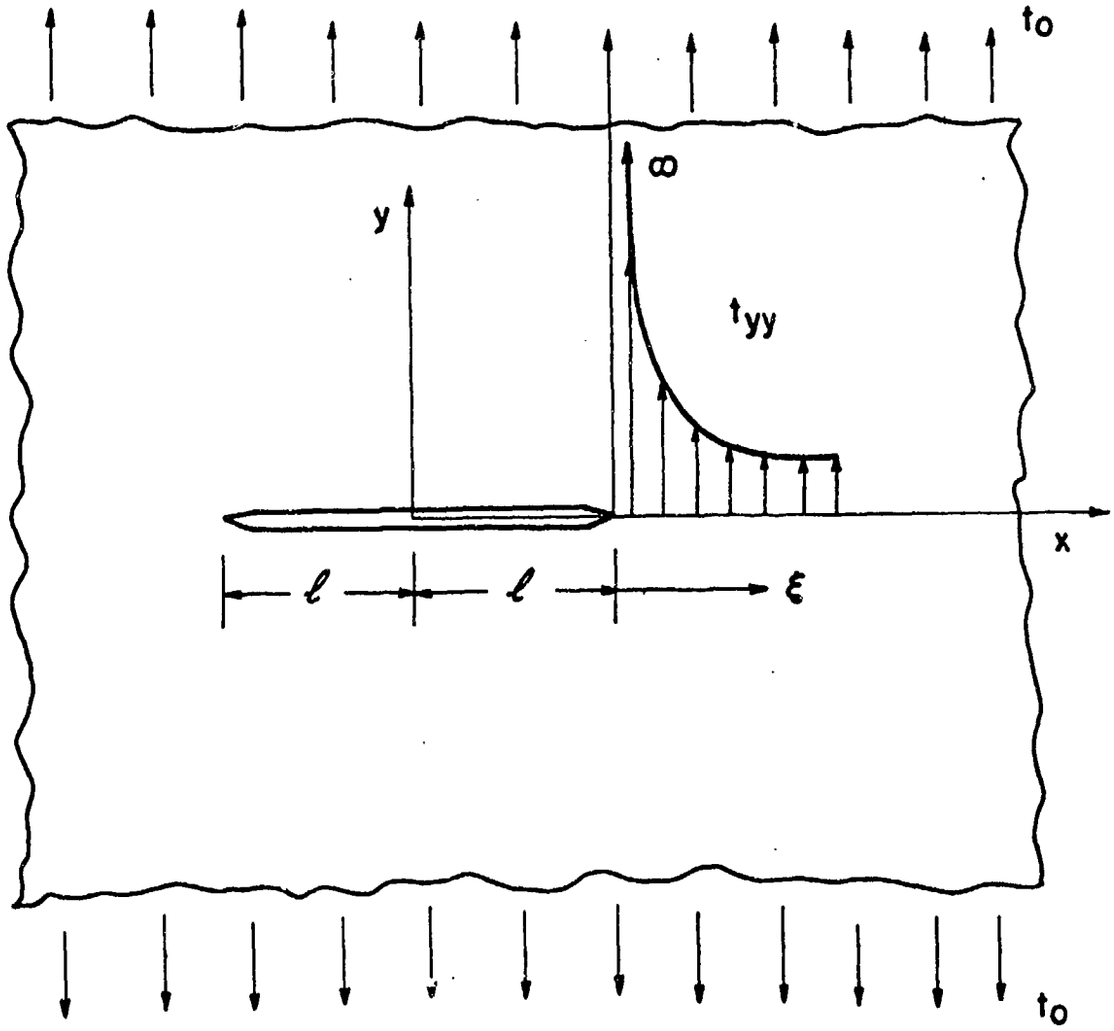

Figure 9

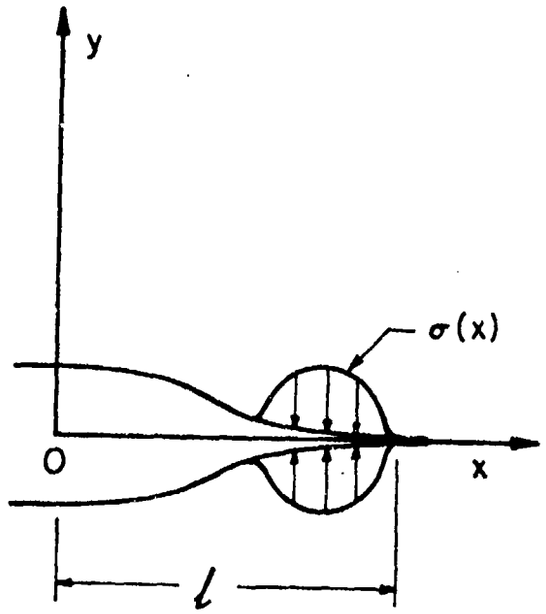

Figure 10

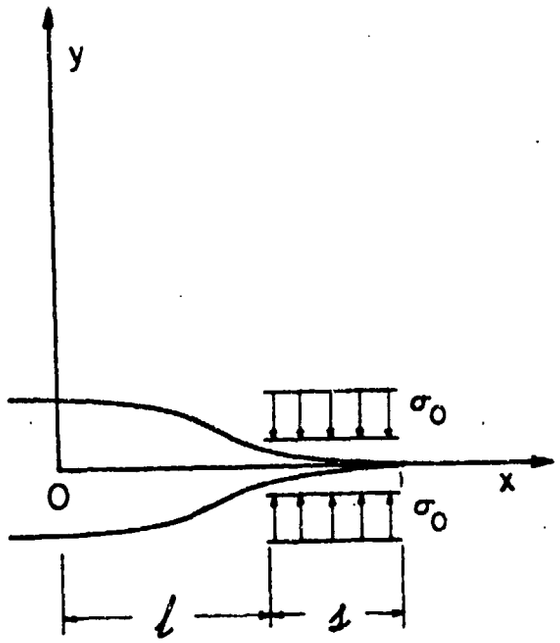

Figure 11

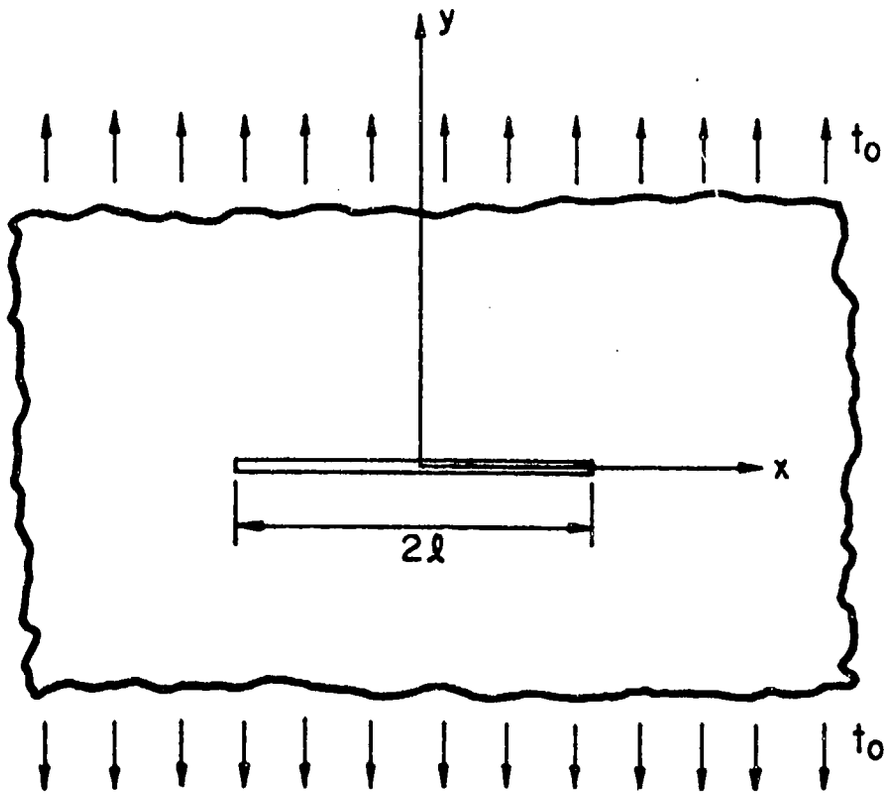

Figure 12

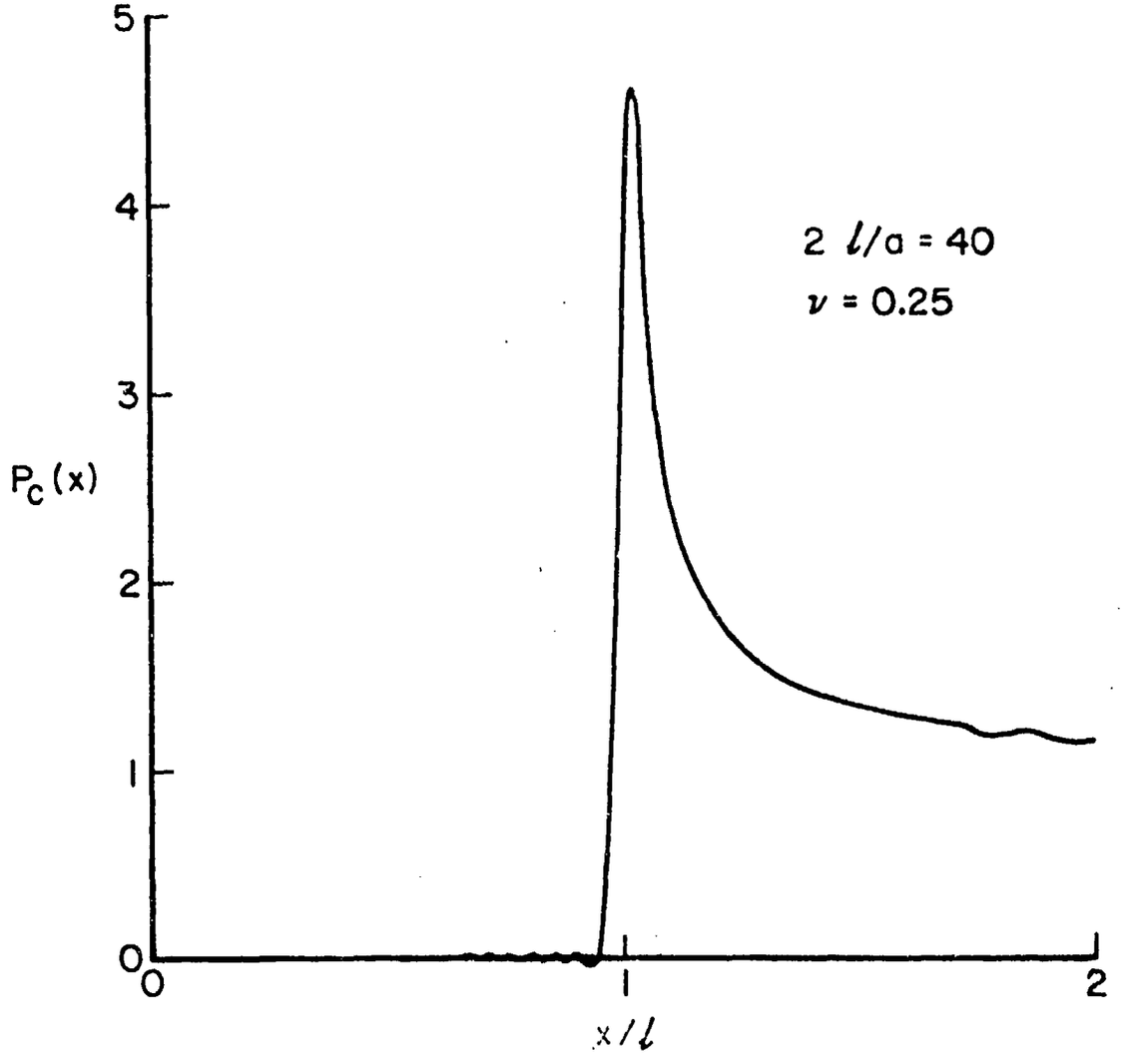

Figure 13

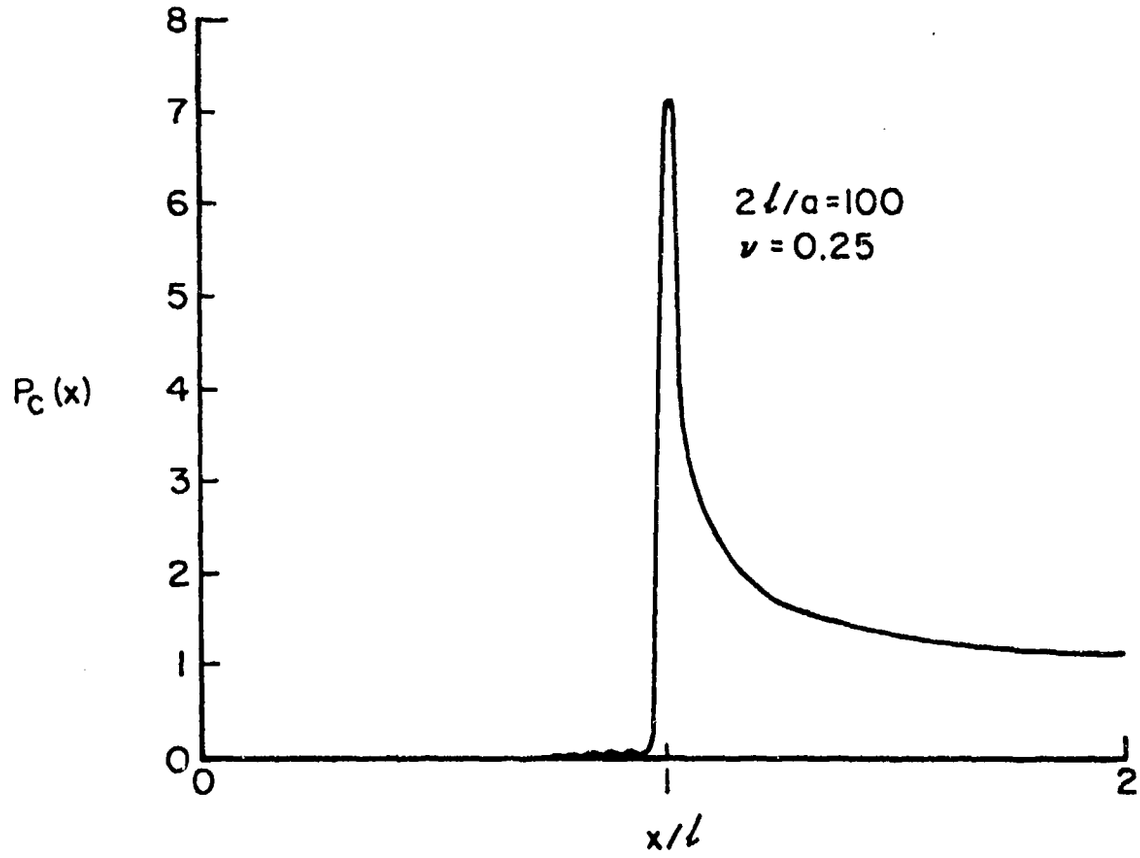

Figure 14

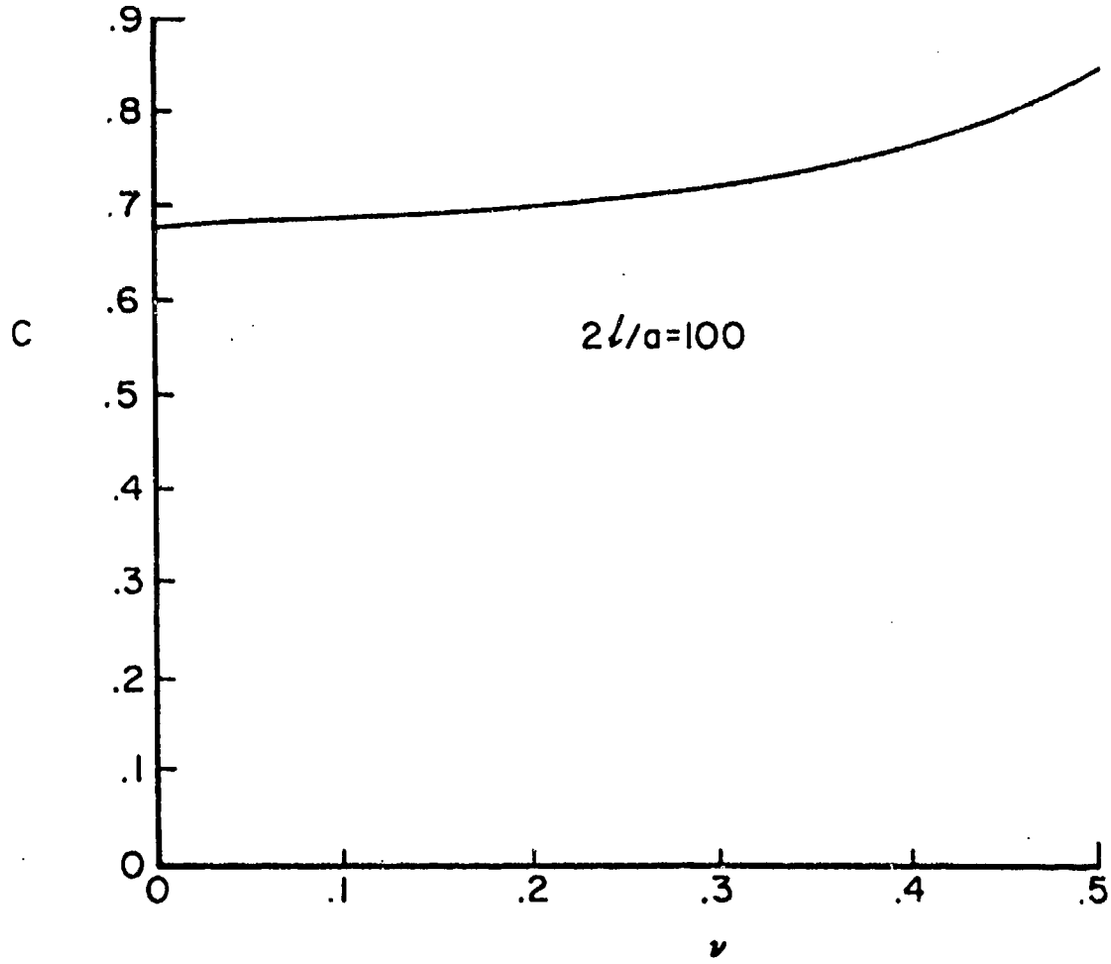

Figure 15

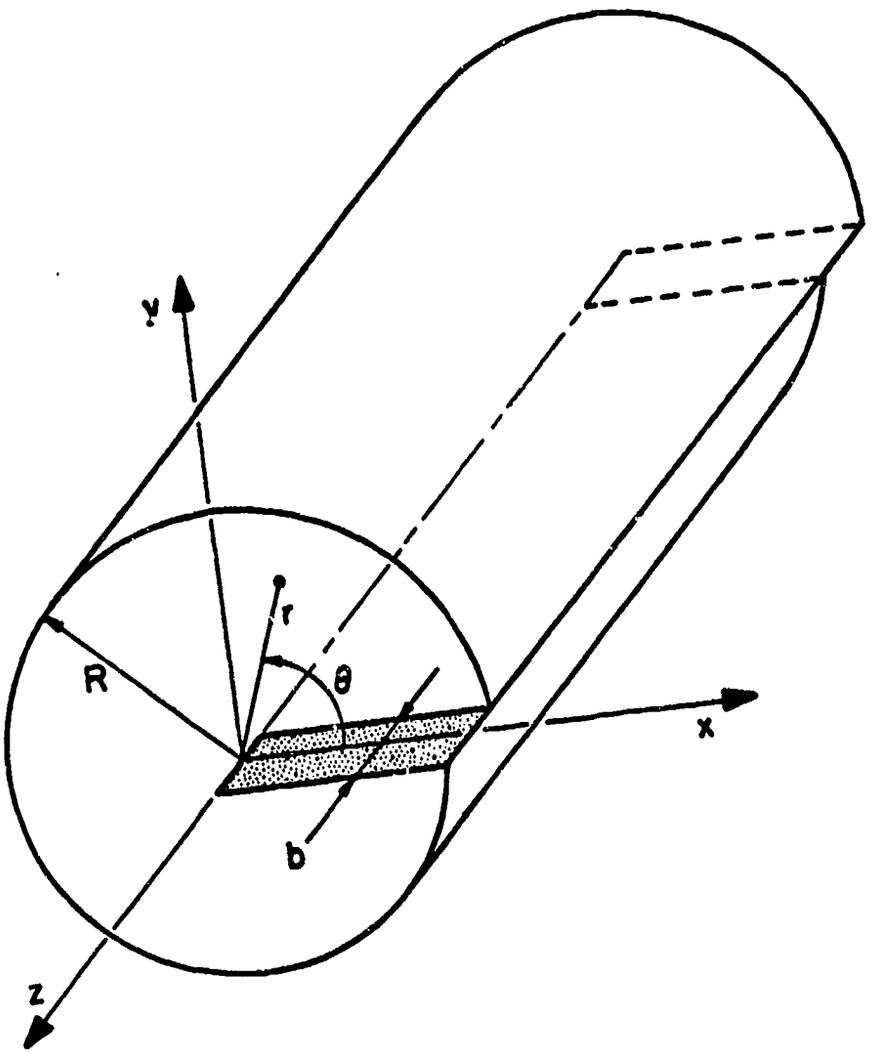

Figure 16

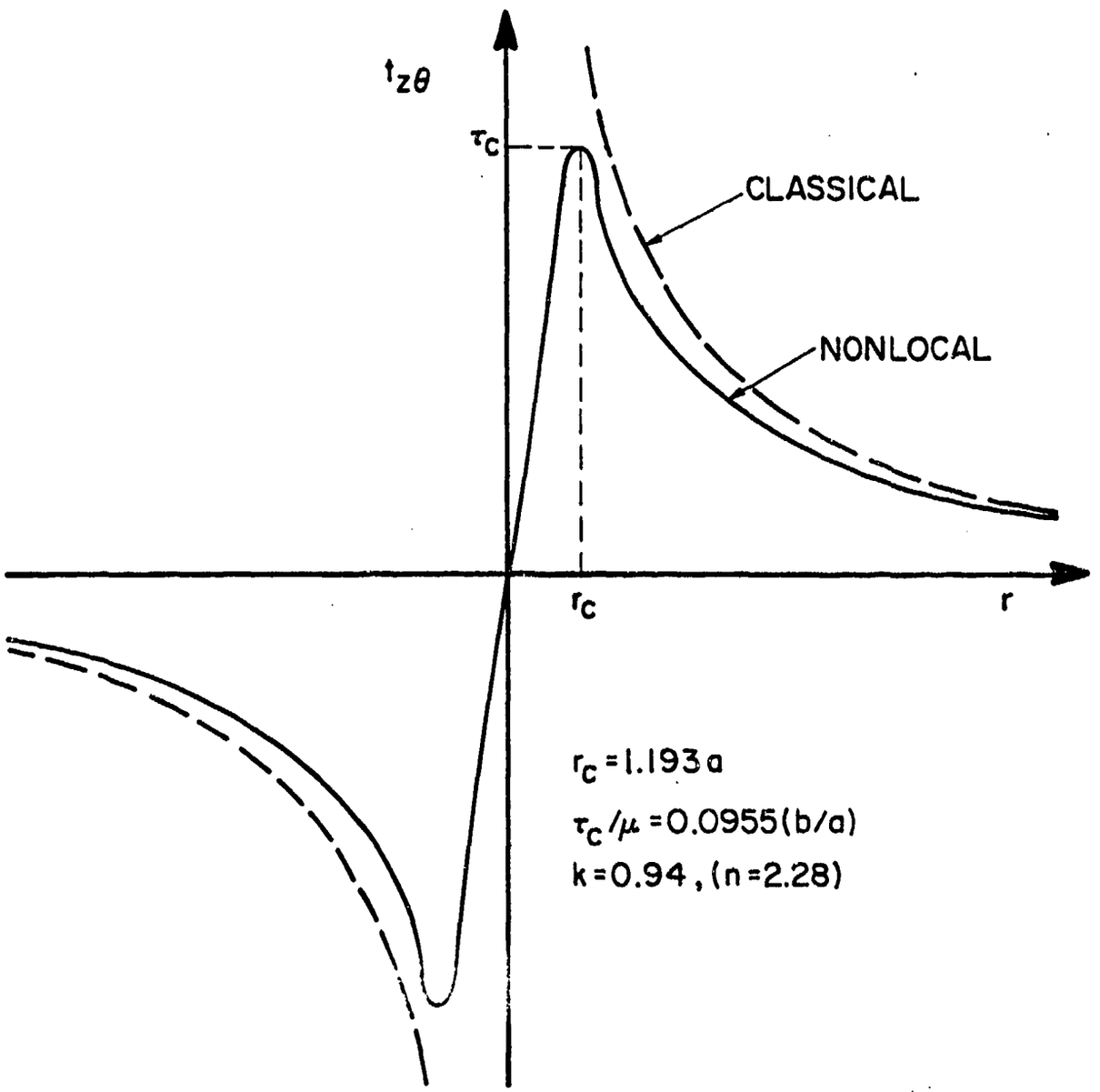
$t_{z\theta}$
τ_c
CLASSICAL
NONLOCAL
r_c
r
$r_c = 1.193a$
$\tau_c/\mu = 0.0955(b/a)$
$k = 0.94$, $(n = 2.28)$

Figure 17

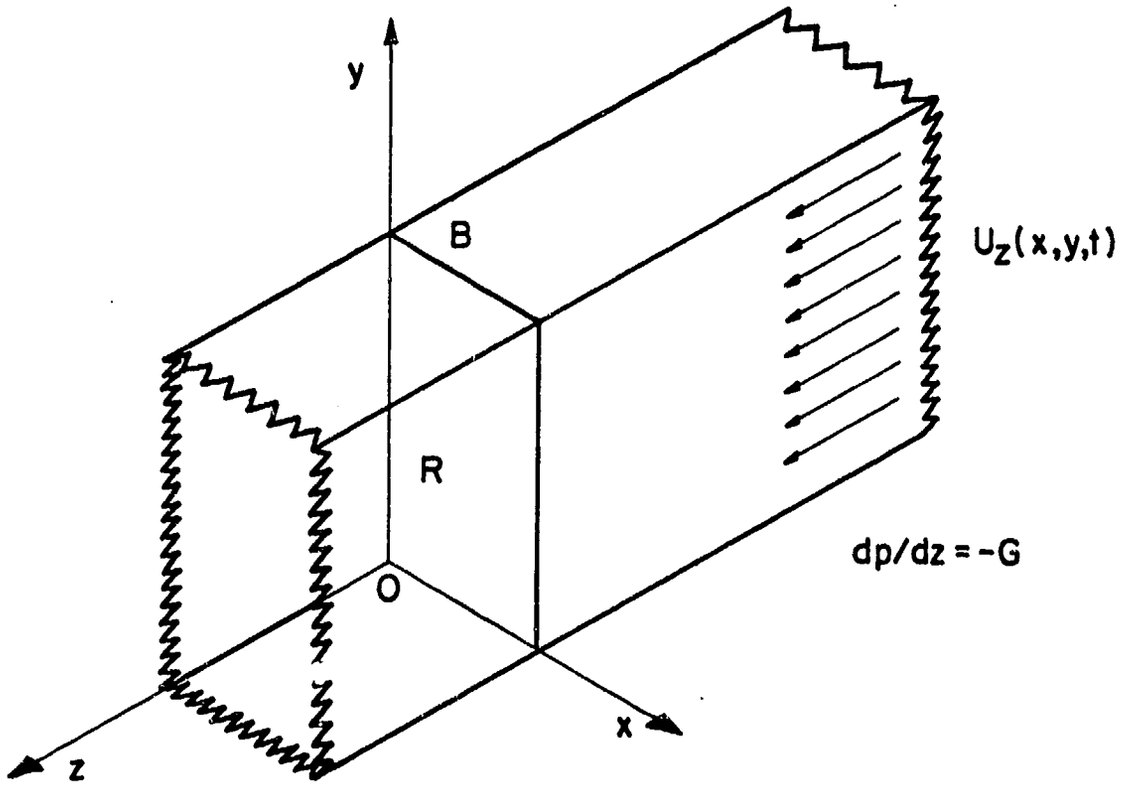

Figure 18

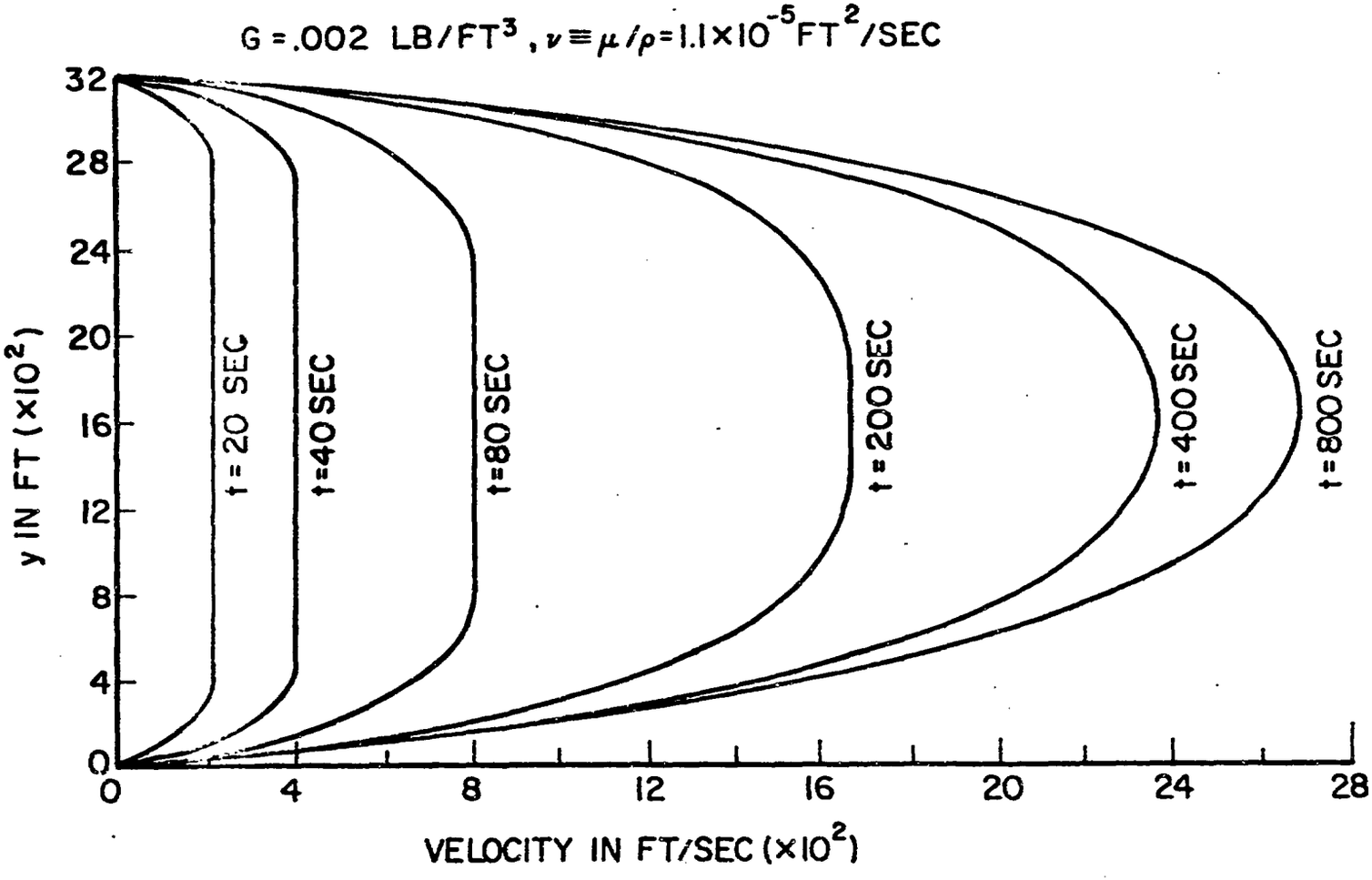
G = .002 LB/FT³, ν ≡ μ/ρ = 1.1×10⁻⁵ FT²/SEC
y IN FT (×10²)
VELOCITY IN FT/SEC (×10²)
t = 20 SEC
t = 40 SEC
t = 80 SEC
t = 200 SEC
t = 400 SEC
t = 800 SEC
0
4
8
12
16
20
24
28
32

Figure 19

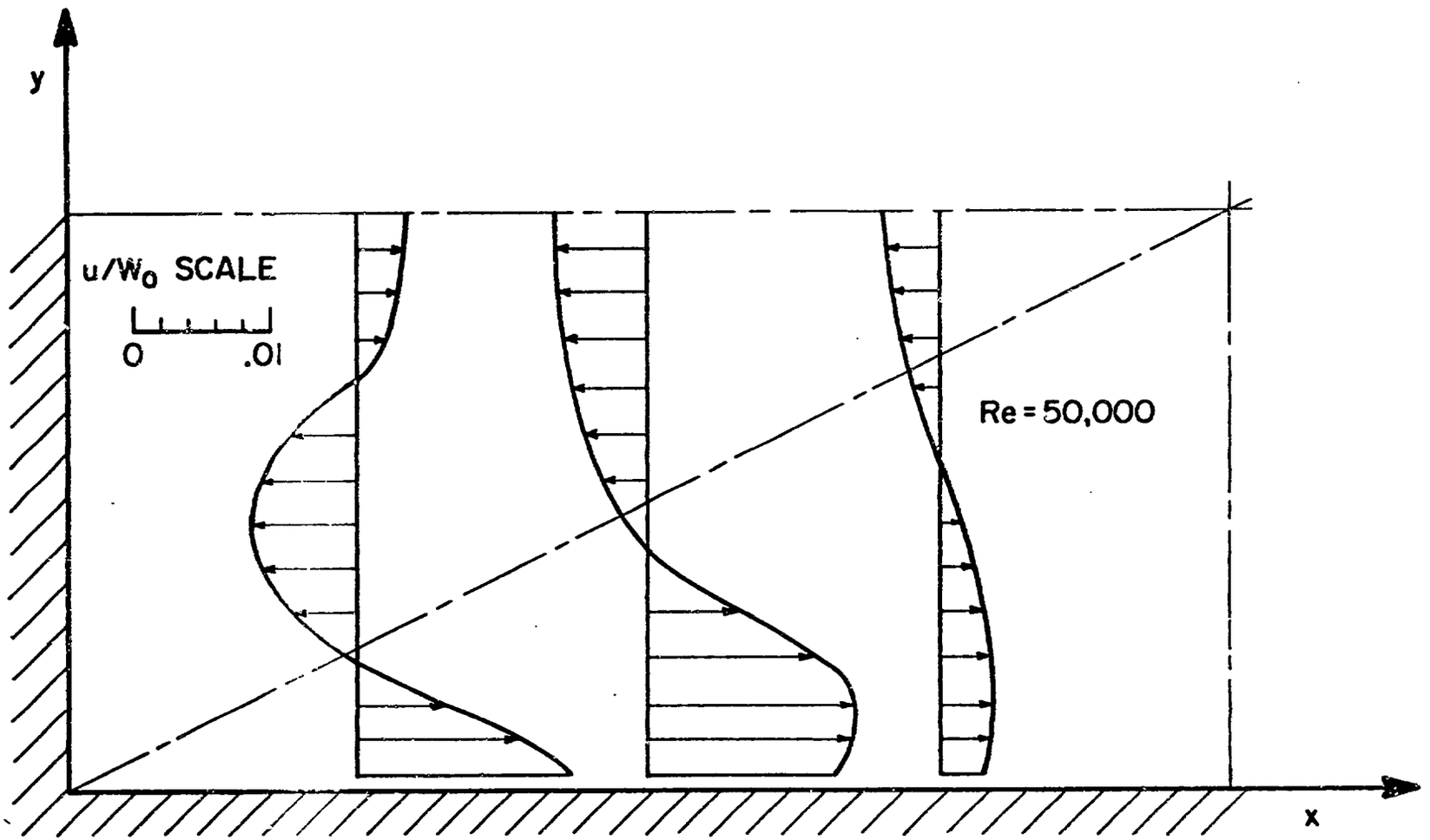

Figure 20

T = 4 SEC

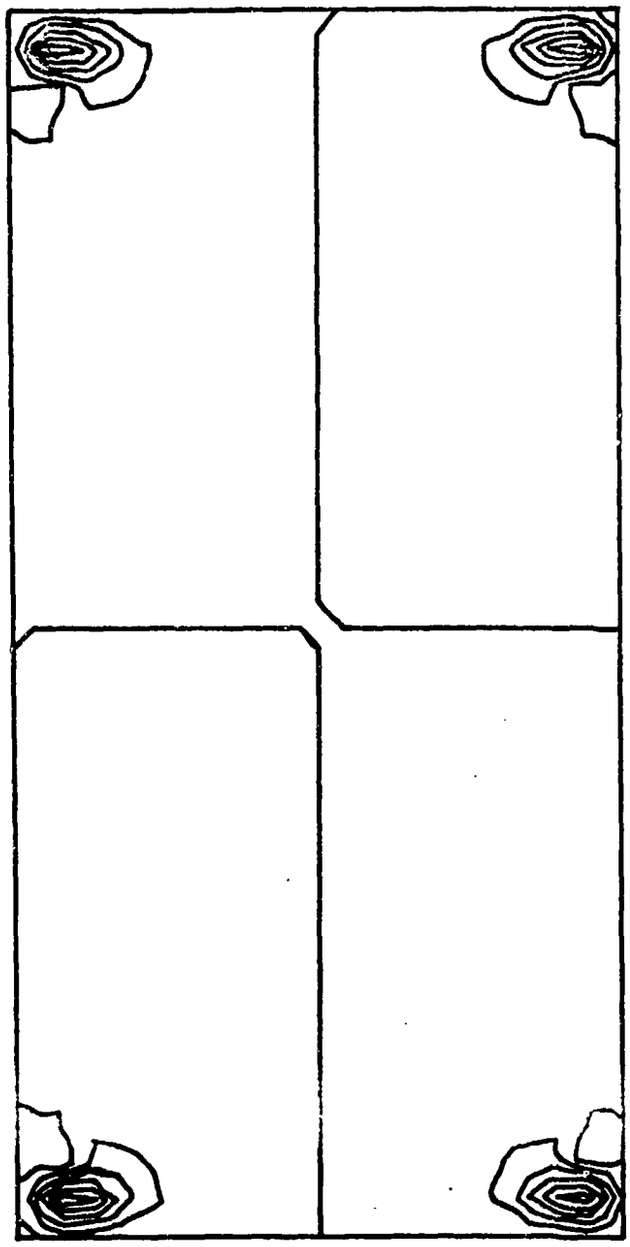

Figure 21

T = 20 SEC

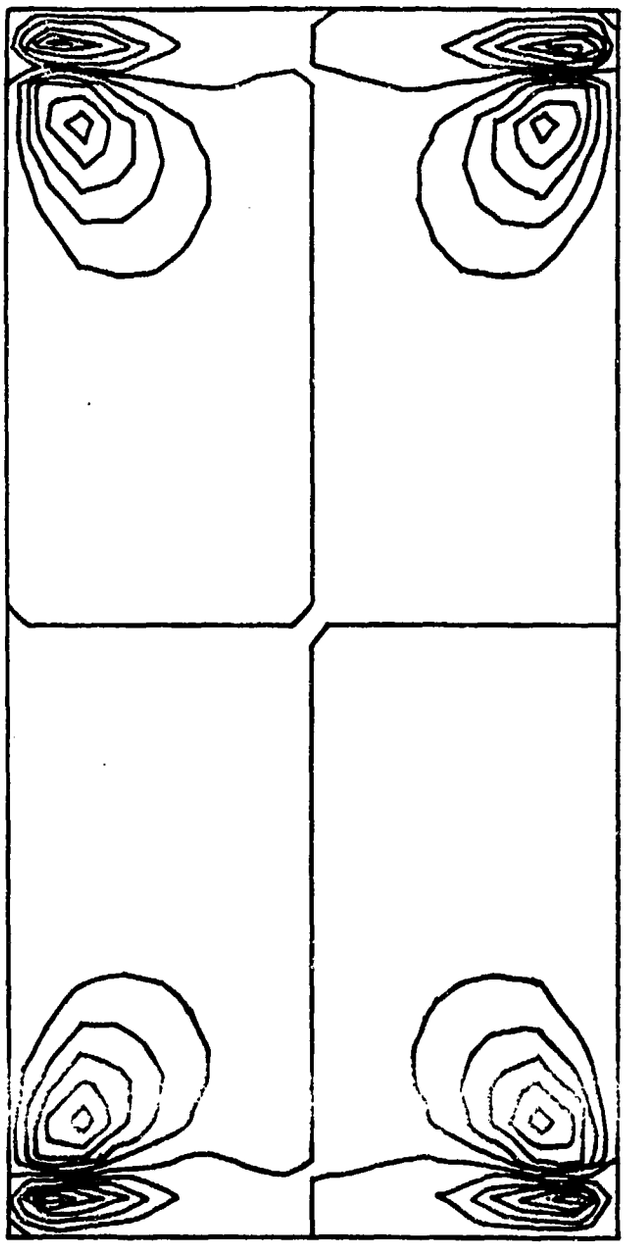

Figure 22

T=60 SEC

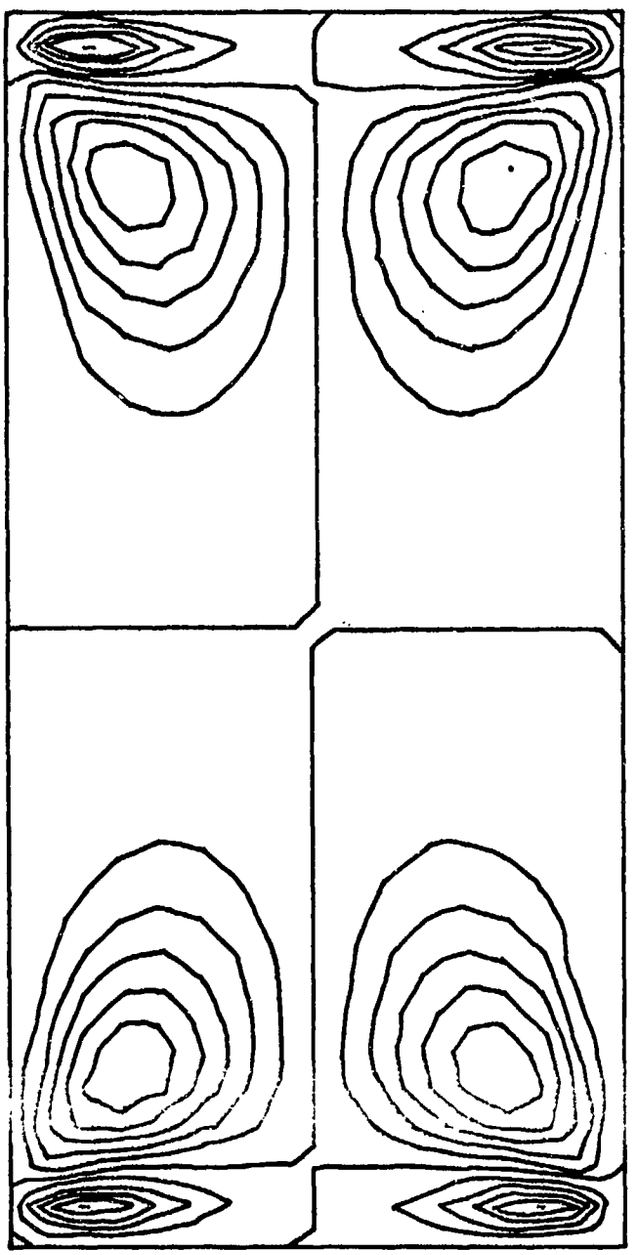

Figure 23

T = 400 SEC

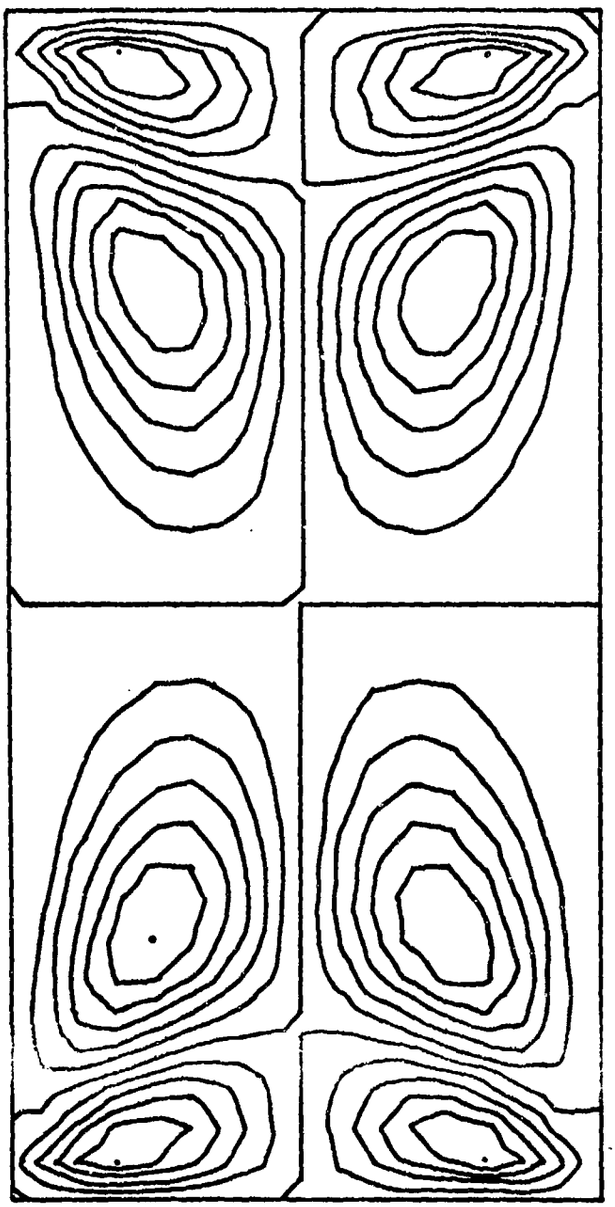

Figure 24

NONLOCAL (STEADY STATE)

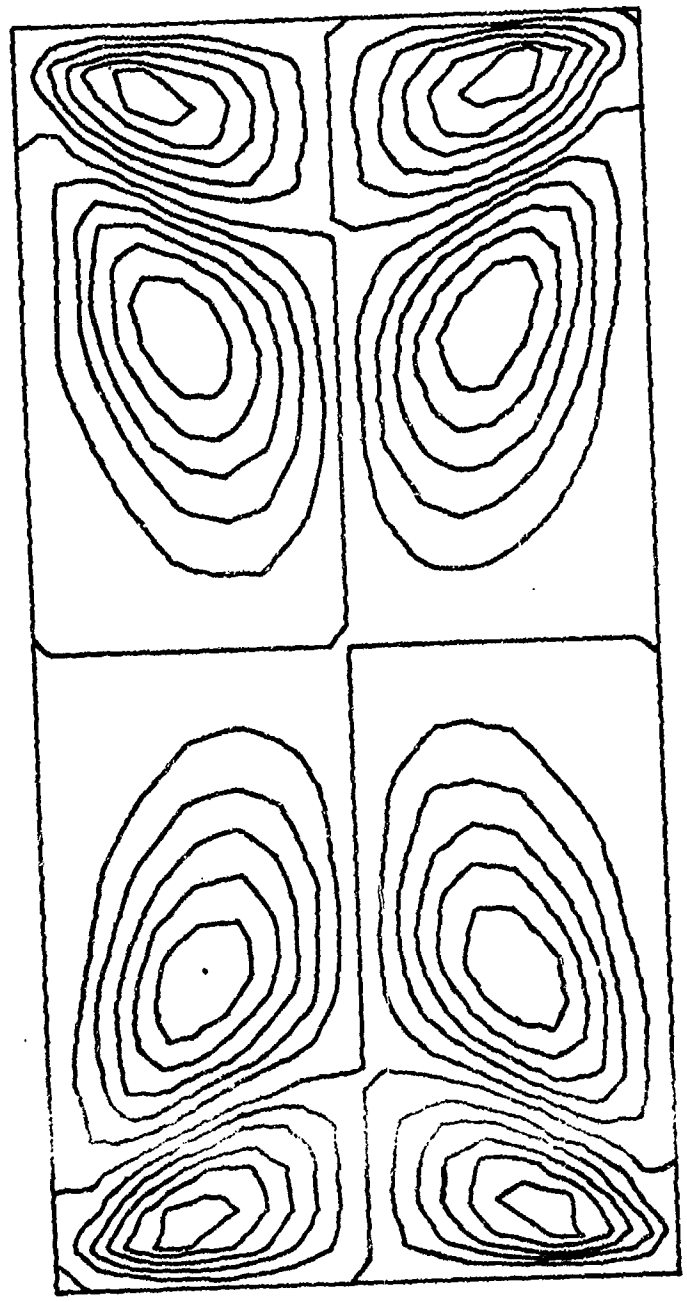

Figure 25

EXPERIMENTAL AFTER NIKURADSE(1926)

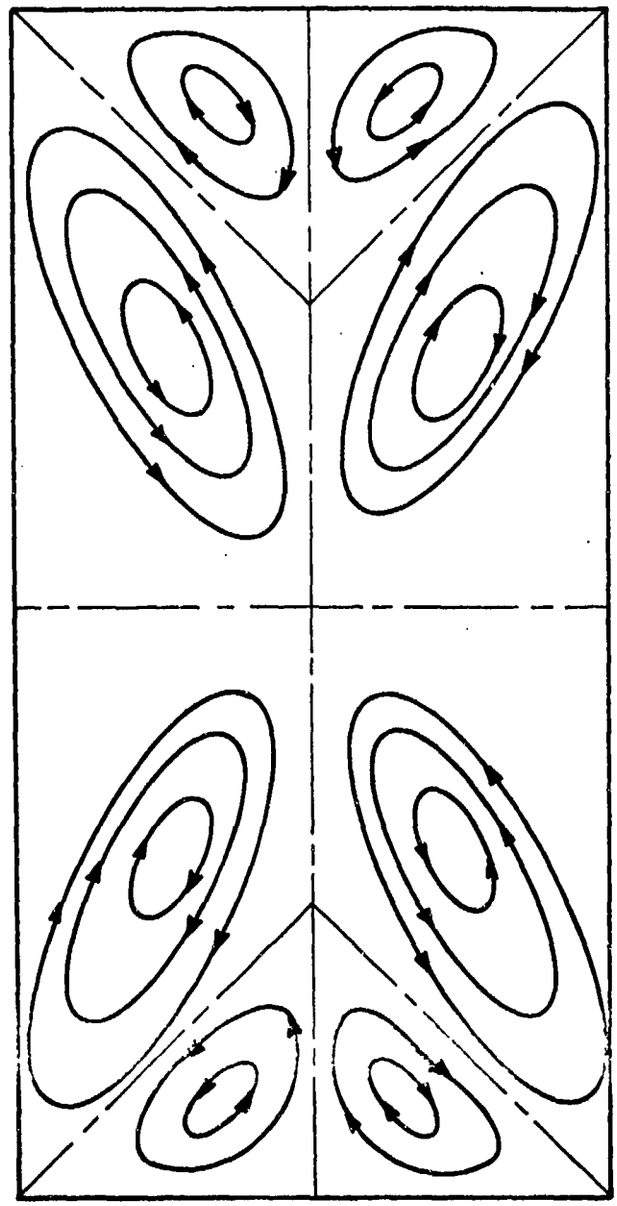

Figure 26

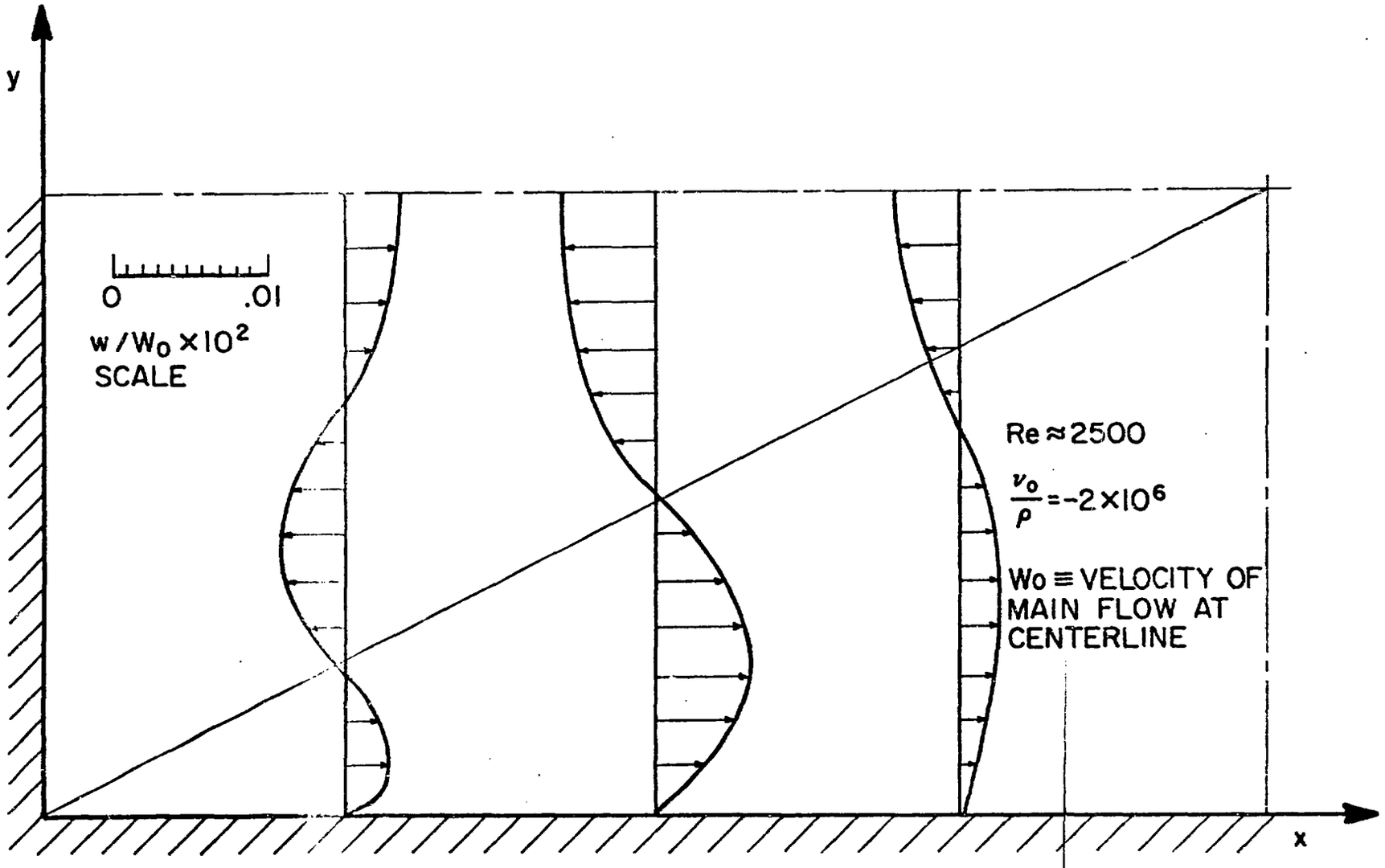
y
0
.01
w/W0 ×10²
SCALE
Re ≈ 2500
ν0/ρ = -2×10⁶
W0 ≡ VELOCITY OF MAIN FLOW AT CENTERLINE
x

Figure 27

PART 1 - GOVERNMENT

Administrative & Liaison Activities

Chief of Naval Research
Department of the Navy
Arlingon, Virginia 22217
Attn: Code 474 (2)
471
222

Director
ONR Branch Office
495 Summer Street
Boston, Massachusetts 02210

Director
ONR Branch Office
219 S. Dearborn Street
Chicago, Illinois 60604

Director
Naval Research Laboratory
Attn: Code 2629 (ONRL)
Washington, D.C. 20390 (6)

U.S. Naval Research Laboratory
Attn: Code 2627
Washington, D.C. 20390

Director
ONR - New York Area Office
715 Broadway - 5th Floor
New York, N.Y. 10003

Director
ONR Branch Office
1030 E. Green Street
Pasadena, California 91101

Defense Documentation Center
Cameron Station
Alexandria, Virginia 22314 (12)

Army

Commanding Officer
U.S. Army Research Office Durham
Attn: Mr. J. J. Murray
CRD-AA-IP
Box CM, Duke Station
Durham, North Carolina 27706 2

Commanding Officer
AMXMR-ATL
Attn: Mr. R. Shea
U.S. Army Materials Res. Agency
Watertown, Massachusetts 02172

Watervliet Arsenal
MAGGS Research Center
Watervliet, New York 12189
Attn: Director of Research

Technical Library

Redstone Scientific Info. Center
Chief, Document Section
U.S. Army Missile Command
Redstone Arsenal, Alabama 35809

Army R&D Center
Fort Belvoir, Virginia 22060

Navy

Commanding Officer and Director
Naval Ship Research & Development Center
Bethesda, Maryland 20034
Attn: Code 042 (Tech. Lib. Br.)
17 (Struc. Mech. Lab.)
172
172
174
177
1800 (Appl. Math. Lab.)
5412S (Dr. W.D. Sette)
19 (Dr. M.M. Sevik)
1901 (Dr. M. Strassberg)
1945
196 (Dr. D Feit)
1962

Naval Weapons Laboratory
Dahlgren, Virginia 22448

Naval Research Laboratory
Washington, D.C. 20375
Attn: Code 8400
8410
8430
8440
6300
6390
6380

Undersea Explosion Research Div.
Naval Ship R&D Center
Norfolk Naval Shipyard
Portsmouth, Virginia 23709
Attn: Dr. E. Palmer
Code 780

Naval Ship Research & Development Center
Annapolis Division
Annapolis, Maryland 21402
Attn: Code 2740 - Dr. Y.F. Wang
28 - Mr. R.J. Wolfe
281 - Mr. R.B. Niederberger
2814 - Dr. H. Vanderveldt

Technical Library
Naval Underwater Weapons Center
Pasadena Annex
3202 E. Foothill Blvd.
Pasadena, California 91107

U.S. Naval Weapons Center
China Lake, California 93557
Attn: Code 4062 - Mr. W. Werback
4520 - Mr. Ken Bischel

Commanding Officer
U.S. Naval Civil Engr. Lab.
Code L31
Port Hueneme, California 93041

Technical Director
U.S. Naval Ordnance Laboratory
White Oak
Silver Spring, Maryland 20910

Technical Director
Naval Undersea R&D Center
San Diego, California 92132

Supervisor of Shipbuilding
U.S. Navy
Newport News, Virginia 23607

Technical Director
Mare Island Naval Shipyard
Vallejo, California 94592

U.S. Navy Underwater Sound Ref. Lab.
Office of Naval Research
P.O. Box 8337
Orlando, Florida 32806

Chief of Naval Operations
Dept. of the Navy
Washington, D.C. 20350
Attn: Code Op07T

Strategic Systems Project Office
Department of the Navy
Washington, D.C. 20390
Attn: NSP-001 Chief Scientist

Deep Submergence Systems
Naval Ship Systems Command
Code 39522
Department of the Navy
Washington, D.C. 20360

Engineering Dept.
U.S. Naval Academy
Annapolis, Maryland 21402

Naval Air Systems Command
Dept. of the Navy
Washington, D.C. 20360
Attn: NAVAIR 5302 Aero & Structures
5308 Structures
52031F Materials
604 Tech. Library
320B Structures

Director, Aero Mechanics
Naval Air Development Center
Johnsville
Warminster, Pennsylvania 18974

Technical Director
U.S. Naval Undersea R&D Center
San Diego, California 92132

Engineering Department
U.S. Naval Academy
Annapolis, Maryland 21402

Naval Facilities Engineering Command
Dept. of the Navy
Washington, D.C. 20360
Attn: NAVFAC 03 Research & Development
04 " "
14114 Tech. Library

Naval Sea Systems Command
Dept. of the Navy
Washington, D.C. 20360
Attn: NAVSHIP 03 Res. & Technology
031 Ch. Scientist for R&
03412 Hydromechanics
037 Ship Silencing Div.
035 Weapons Dynamics

Naval Ship Engineering Center
Prince George's Plaza
Hyattsville, Maryland 20782
Attn: NAVSEC 6100 Ship Sys Engr & Des Dep
6102C Computer-Aided Ship Des
6105G
6110 Ship Concept Design
6120 Hull Div.
6120D Hull Div.
6128 Surface Ship Struct.
6129 Submarine Struct.

Air Force

Commander WADD
Wright-Patterson Air Force Base
Dayton, Ohio 45433
Attn: Code WWRMDD
AFFDL (FDDS)
Structures Division
AFLC (MCEEA)

Chief, Applied Mechanics Group
U.S. Air Force Inst. of Tech.
Wright-Patterson Air Force Base
Dayton, Ohio 45433

Chief, Civil Engineering Branch
WLRC, Research Division
Air Force Weapons Laboratory
Kirtland AFB, New Mexico 87117

Air Force Office of Scientific Research
1400 Wilson Blvd.
Arlington, Virginia 22209
Attn: Mechanics Div.

NASA

Structures Research Division
National Aeronautics & Space Admin.
Langley Research Center
Langley Station
Hampton, Virginia 23365

National Aeronautic & Space Admin.
Associate Administrator for Advanced
Research & Technology
Washington, D.C. 02546

Scientific & Tech. Info. Facility
NASA Representative (S-AK/DL)
P.O. Box 5700
Bethesda, Maryland 20014

Other Government Activities

Commandant
Chief, Testing & Development Div.
U.S. Coast Guard
1300 E. Street, N.W.
Washington, D.C. 20226

Technical Director
Marine Corps Dev. & Educ. Command
Quantico, Virginia 22134

Director
National Bureau of Standards
Washington, D.C. 20234
Attn: Mr. B.L. Wilson, EM 219

Dr. M. Gaus
National Science Foundation
Engineering Division
Washington, D.C. 20550

Science & Tech. Division
Library of Congress
Washington, D.C. 20540

Director
Defense Nuclear Agency
Washington, D.C. 20305
Attn: SPSS

Commander Field Command
Defense Nuclear Agency
Sandia Base
Albuquerque, New Mexico 87115

Director Defense Research & Engrg
Technical Library
Room 3C-128
The Pentagon
Washington, D.C. 20301

Chief, Airframe & Equipment Branch
FS-120
Office of Flight Standards
Federal Avaiation Agency
Washington, D.C. 20553

Chief, Research and Development
Maritime Administration
Washington, D.C. 20235

Deputy Chief, Office of Ship Constr.
Maritime Administration
Washington, D.C. 20235
Attn: Mr. U.L. Russo

Atomic Energy Commission
Div. of Reactor Devel. & Tech.
Germantown, Maryland 20767

Ship Hull Research Committee
National Research Council
National Academy of Sciences
2101 Constitution Avenue
Washington, D.C. 20418
Attn: Mr. A.R. Lytle

PART 2 - CONTRACTORS AND OTHER TECHNICAL COLLABORATORS

Universities

Dr. J. Tinsley Oden
University of Texas at Austin
345 Eng. Science Bldg.
Austin, Texas 78712

Prof. Julius Miklowitz
California Institute of Technology
Div. of Engineering & Applied Sciences
Pasadena, California 91109

Dr. Harold Liebowitz, Dean
School of Engr. & Applied Science
George Washington University
725 - 23rd St., N.W.
Washington, D.C. 20006

Prof. Eli Sternberg
California Institute of Technology
Div. of Engr. & Applied Sciences
Pasadena, California 91109

Prof. Paul M. Naghdi
University of California
Div. of Applied Mechanics
Etcheverry Hall
Berkeley, California 94720

Professor P. S. Symonds
Brown University
Division of Engineering
Providnece, R.I. 02912

Prof. A. J. Durelli
The Catholic University of America
Civil/Mechanical Engineering
Washington, D.C. 20017

Prof. R.B. Testa
Columbia University
Dept. of Civil Engineering
S.W. Mudd Bldg.
New York, N.Y. 10027

Prof. H. H. Bleich
Columbia University
Dept. of Civil Engineering
Amsterdam & 120th St.
New York, N.Y. 10027

Prof. F.L. DiMaggio
Columbia University
Dept. of Civil Engineering
616 Mudd Building
New York, N.Y. 10027

Prof. A.M. Freudenthal
George Washington University
School of Engineering & Applied Science
Washington, D.C. 20006

D. C. Evans
University of Utah
Computer Science Division
Salt Lake City, Wash 84112

Prof. Norman Jones
Massachusetts Inst. of Technology
Dept. of Naval Architecture & Marine Engrng
Cambridge, Massachusetts 02139

Professor Albert I. King
Biomechanics Research Center
Wayne State University
Detroit, Michigan 48202

Dr. V. R. Hodgson
Wayne State University
School of Medicine
Detroit, Michigan 48202

Dean B. A. Boley
Northwestern University
Technological Institute
2145 Sheridan Road
Evanston, Illinois 60201

Prof. P.G. Hodge, Jr.
University of Minnesota
Dept. of Aerospace Engng & Mechanics
Minneapolis, Minnesota 55455

Dr. D.C. Drucker
University of Illinois
Dean of Engineering
Urbana, Illinois 61801

Prof. N.M. Newmark
University of Illinois
Dept. of Civil Engineering
Urbana, Illinois 61801

Prof. E. Reissner
University of California, San Diego
Dept. of Applied Mechanics
La Jolla, California 92037

Prof. William A. Nash
University of Massachusetts
Dept. of Mechanics & Aerospace Engng.
Amherst, Massachusetts 01002

Library (Code 0384)
U.S. Naval Postgraduate School
Monterey, California 93940

Prof. Arnold Allentuch
Newark College of Engineering
Dept. of Mechanical Engineering
323 High Street
Newark, New Jersey 07102

Dr. George Herrmann
Stanford University
Dept. of Applied Mechanics
Stanford, California 94305

Prof. J. D. Achenbach
Northwestern University
Dept. of Civil Engineering
Evanston, Illinois 60201

Director, Applied Research Lab.
Pennsylvania State University
P. O. Box 30
State College, Pennsylvania 16801

Prof. Eugen J. Skudrzyk
Pennsylvania State University
Applied Research Laboratory
Dept. of Physics - P.O. Box 30
State College, Pennsylvania 16801

Prof. J. Kempner
Polytechnic Institute of Brooklyn
Dept. of Aero.Engrg.& Applied Mech
333 Jay Street
Brooklyn, N.Y. 11201

Prof. J. Klosner
Polytechnic Institute of Brooklyn
Dept. of Aerospace & Appl. Mech.
333 Jay Street
Brooklyn, N.Y. 11201

Prof. R.A. Schapery
Texas A&M University
Dept. of Civil Engineering
College Station, Texas 77840

Prof. W.D. Pilkey
University of Virginia
Dept. of Aerospace Engineering
Charlottesville, Virginia 22903

Dr. H.G. Schaeffer
University of Maryland
Aerospace Engineering Dept.
College Park, Maryland 20742

Prof. K.D. Willmert
Clarkson College of Technology
Dept. of Mechanical Engineering
Potsdam, N.Y. 13676

Dr. J.A. Stricklin
Texas A&M University
Aerospace Engineering Dept.
College Station, Texas 77843

Dr. L.A. Schmit
University of California, LA
School of Engineering & Applied Science
Los Angeles, California 90024

Dr. H.A. Kamel
The University of Arizona
Aerospace & Mech. Engineering Dept.
Tucson, Arizona 85721

Dr. B.S. Berger
University of Maryland
Dept. of Mechanical Engineering
College Park, Maryland 20742

Prof. G. R. Irwin
Dept. of Mechanical Engrg.
University of Maryland
College Park, Maryland 20742

Dr. S.J. Fenves
Carnegie-Mellon University
Dept. of Civil Engineering
Schenley Park
Pittsburgh, Pennsylvania 15213

Dr. Ronald L. Huston
Dept. of Engineering Analysis
Mail Box 112
University of Cincinnati
Cincinnati, Ohio 45221

Prof. George Sih
Dept. of Mechanics
Lehigh University
Bethlehem, Pennsylvania 18015

Prof. A.S. Kobayashi
University of Washington
Dept. of Mechanical Engineering
Seattle, Washington 98105

Librarian
Webb Institute of Naval Architecture
Crescent Beach Road, Glen Cove
Long Island, New York 11542

Prof. Daniel Frederick
Virginia Polytechnic Institute
Dept. of Engineering Mechanics
Blacksburg, Virginia 24061

Prof. A.C. Eringen
Dept. of Aerospace & Mech. Sciences
Princeton University
Princeton, New Jersey 08540

Dr. S.L. Koh
School of Aero., Astro.& Engr. Sc.
Purdue University
Lafayette, Indiana 47907

Prof. E.H. Lee
Div. of Engrg. Mechanics
Stanford University
Stanford, California 94305

Prof. R.D. Mindlin
Dept. of Civil Engrg.
Columbia University
S.W. Mudd Building
New York, N.Y. 10027

Prof. S.B. Dong
University of California
Dept. of Mechanics
Los Angeles, California 90024

Prof. Burt Paul
University of Pennsylvania
Towne School of Civil & Mech. Engrg.
Rm. 113 - Towne Building
220 S. 33rd Street
Philadelphia, Pennsylvania 19104

Prof. H.W. Liu
Dept. of Chemical Engr. & Metal.
Syracuse University
Syracuse, N.Y. 13210

Prof. S. Bodner
Technion R&D Foundation
Haifa, Israel

Prof. R.J.H. Bollard
Chairman, Aeronautical Engr. Dept.
207 Guggenheim Hall
University of Washington
Seattle, Washington 98105

Prof. G.S. Heller
Division of Engineering
Brown University
Providence, Rhode Island 02912

Prof. Werner Goldsmith
Dept. of Mechanical Engineering
Div. of Applied Mechanics
University of California
Berkeley, California 94720

Prof. J.R.Rice
Division of Engineering
Brown University
Providence, Rhode Island 02912

Prof. R.S. Rivlin
Center for the Application of Mathematics
Lehigh University
Bethlehem, Pennsylvania 18015

Library (Code 0384)
U.S. Naval Postgraduate School
Monterey, California 93940

Dr. Francis Cozzarelli
Div. of Interdisciplinary
Studies & Research
School of Engineering
State University of New York
Buffalo, N.Y. 14214

Industry and Research Institutes

Library Services Department
Report Section Bldg. 14-14
Argonne National Laboratory
9700 S. Cass Avenue
Argonne, Illinois 60440

Dr. M. C. Junger
Cambridge Acoustical Associates
129 Mount Auburn St.
Cambridge, Massachusetts 02138

Dr. L.H. Chen
General Dynamics Corporation
Electric Boat Division
Groton, Connecticut 06340

Dr. J.E. Greenspon
J.G. Engineering Research Associates
3831 Menlo Drive
Baltimore, Maryland 21215

Dr. S. Batdorf
The Aerospace Corp.
P.O. Box 92957
Los Angeles, California 90009

Dr. K.C. Park
Lockheed Palo Alto Research Laboratory
Dept. 5233, Bldg. 205
3251 Hanover Street
Palo Alto, CA 94304

Library
Newport News Shipbuilding &
Dry Dock Company
Newport News, Virginia 23607

Dr. W.F. Bozich
McDonnell Douglas Corporation
5301 Bolsa Ave.
Huntington Beach, CA 92647

Dr. H.N. Abramson
Southwest Research Institute
Technical Vice President
Mechanical Sciences
P.O. Drawer 28510
San Antonio, Texas 78284

Dr. R.C. DeHart
Southwest Research Institute
Dept. of Structural Research
P.O. Drawer 28510
San Antonio, Texas 78284

Dr. M.L. Baron
Weidlinger Associates,
Consulting Engineers
110 East 59th Street
New York, N.Y. 10022

Dr. W.A. von Riesemann
Sandia Laboratories
Sandia Base
Albuquerque, Ney Mexico 87115

Dr. T.L. Geers
Lockheed Missiles & Space Co.
Palo Alto Research Laboratory
3251 Hanover Street
Palo Alto, California 94304

Dr. J.L. Tocher
Boeing Computer Services, Inc.
P.O. Box 24346
Seattle, Washington 98124

Mr. Willian Caywood
Code BBE, Applied Physics Laboratory
8621 Georgia Avenue
Silver Spring, Maryland 20034

Mr. P.C. Durup
Lockheed-California Company
Aeromechanics Dept., 74-43
Burbank, California 91503